REPORT DOCUMENTATION PAGE

Form Approved
OMB No. 0704-0188

PLEASE DO NOT RETURN YOUR FORM TO THE ABOVE ORGANIZATION.

1. REPORT DATE *(DD-MM-YYYY)*	2. REPORT TYPE	3. DATES COVERED *(From - To)*
20-07-2006	Final report	From 15 March 2005 to 15 March 2006

4. TITLE AND SUBTITLE
Miniature Electron Sources for Tomorrow's vacuum THz Devices (MiPRI)

5a. CONTRACT NUMBER

5b. GRANT NUMBER
FA9550-05-1-0190

5c. PROGRAM ELEMENT NUMBER

6. AUTHOR(S)
Carmel, Yuval
Nusinovich, Gregory
Rodgers, John
Shkvarunets, Anatoly

5d. PROJECT NUMBER

5e. TASK NUMBER

5f. WORK UNIT NUMBER

7. PERFORMING ORGANIZATION NAME(S) AND ADDRESS(ES)
Institute for Research in Electronic and Applied Physics
University of Maryland
College Park, MD 20742

8. PERFORMING ORGANIZATION REPORT NUMBER

9. SPONSORING/MONITORING AGENCY NAME(S) AND ADDRESS(ES)
Dr. Robert J. Barker
AFOSR/NE
875 N. Randolph Street, Rm 3-112
Arlington, VA 22203-1768
(703) 696-8574, fax (703) 696-8481

10. SPONSOR/MONITOR'S ACRONYM(S)
AFOSR

11. SPONSOR/MONITOR'S REPORT

AFRL-SR-AR-TR-06-0330

12. DISTRIBUTION/AVAILABILITY STATEMENT
Distribution Statement A: unlimited

13. SUPPLEMENTARY NOTES

14. ABSTRACT
The most significant experimental accomplishment was the demonstration that plasma-assisted miniature cathodes can generate high perveance electron beams at low voltages (>1000A/cm2; 0.5-3kV), and that those beams could propagate without external guiding magnetic fields over distances compatible with the length of the RF structure of THz sources. Out theoretical studies showed that this will enable the design of future THz sources operating with relatively high efficiency at high power levels.

15. SUBJECT TERMS
THz, plasma assisted cathodes, high perveance electron beam, miniature electron sources

16. SECURITY CLASSIFICATION OF:			17. LIMITATION OF ABSTRACT	18. NUMBER OF PAGES	19a. NAME OF RESPONSIBLE PERSON
a. REPORT	b. ABSTRACT	c. THIS PAGE			19b. TELEPHONE NUMBER *(Include area code)*

INSTITUTE FOR RESEARCH IN
ELECTRONICS
& APPLIED PHYSICS

MINIATURE ELECTRON SOURCES FOR TOMORROW'S VACUUM THz DEVICES (MiPRI)

Final Report for the period 3/15/05-3/14/06

AFOSR Grant Number FA95500510190

Submitted to

Dr. R. Barker
Air Force Office of Scientific Research

Work performed by

Institute for Research in Electronics and Applied Physics
University of Maryland
College Park, MD 20742-3511

July 2006

Table of content

Introduction and identification of the challenges

There has been a recent explosion of interest in using terahertz (THz) radiation to various applications in chemistry, biology, physics (spectroscopy), medicine, material science and imaging. This interest is motivated by the fact that the THz part of the spectrum is energetically equivalent to many physical, chemical and biological processes. Simultaneously there has been a rapid development of a broad array of experimental tools for working with THz radiation. With the advent of modern micro-fabrication and MEMS technologies, the operating frequencies of vacuum electron microwave devices are being extended into the THz regions. One example, a 1 THz Backward Wave Oscillator (BWO) is commercially available[1]. However, state-of-the-art THz BWOs are inefficient (<0.001%) and very heavy (>350kg, including required magnets and power supplies), making them impractical for widespread applications.

Extending microwave sources into the sub-mm wave region, combined with the need for miniaturization, poses a variety of very serious challenges for electron cathode performance, as well as for electron beam transport, quality and focusing. Extending the frequency to the THz range requires confining the electron beam to an increasingly small cross section. In fact, since the required beam current density is proportional to the operating frequency squared[2], the challenge is to generate and realize in the interaction space the extremely high current densities ($\sim 10^3 A/cm^2$) required even for low power (~0.1W) sources. A second challenge is to overcome the traditional reliance on bulky magnets and solenoids needed for magnetic confinement of electron beams.

Achieving the desired electron beam current density needed for compact vacuum THz sources is very challenging. Explosive emission cathodes offer high current density, but suffer from short pulse length (typically <1μsec), poor beam quality and fast deterioration of electrodes. Conventional thermionic cathodes widely used in the microwave tube industry can provide long pulse operation, but typically are limited to low current density ($\leq 10\ A/cm^2$).

In this research program we investigated a novel approach to fill the need for advanced, miniaturized, plasma-assisted electron sources suitable for tomorrow's THz microwave vacuum (MVE) systems. To establish the context, let us note that there are some alternative concepts of electron guns proposed for THz sources. The approach investigated in this research program includes two significant innovations:

1) the use of a miniaturized, long lived, high current density, plasma-assisted electron sources, and

2) the accompanying use of ion focusing to eliminate the need for heavy focusing magnets and improve the quality of the electron beam.

Plasma-assisted cathodes look attractive because of their ability to produce high current densities. They can be considered "equivalent" to indestructible thermionic cathodes operating at effective temperature ~20,000^{0}C having a zero work function

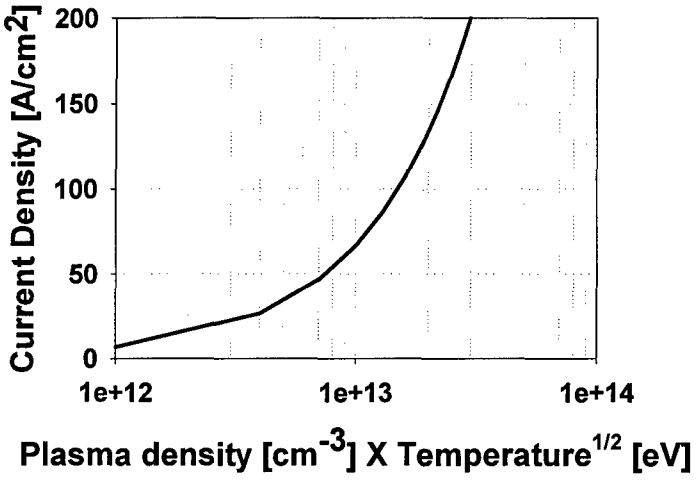

Fig. 1. Plasma-assisted cathodes are characterized by very high current density capability, as needed for THz sources.

without perveance limits, that do not exist in the plasma. For example, Fig. 1 illustrates the calculated maximum current density from plasma-assisted cathodes under various conditions. This figure describes a hypothetical situation where all available electrons are extracted from the plasma. A limit of 200 A/cm^2 corresponds to a $1.5 \cdot 10^{13}$ cm^{-3}, 2eV plasma.

Plasma-assisted cathodes can be compatible with high-vacuum technology necessary for THz sources; a short discussion of this topic is in order. The "common wisdom" is that plasma-assisted cathodes are fundamentally incompatible with extreme vacuum conditions because they require a gas pressure ~10^{-4} Torr, which is prohibitively high for conventional vacuum devices. Note, however, that practically all vacuum microwave devices contain some amount of plasma. So the issue is therefore not the plasma itself, but rather how much plasma is acceptable. As long as the plasma frequency of the plasma in the interaction space of a device is much less than the operating frequency ($\omega_p << \omega$ or, more exactly, $\omega_p^2 << \omega^2$), the device can be practically considered as a vacuum device. Since in the THz frequency range the operating frequency is much higher than the frequency of conventional L-band or S-band microwave devices, this condition can be easily satisfied in THz frequency band, even in the presence of a background gas with the pressure on the order of 10^{-4} Torr, as shown in Table 1.

Table 1: THz MVE devices driven by plasma-assisted cathodes can be compatible with vacuum electronic device technology.

	GHz MVE devices driven by thermionic cathodes	**THz MVE devices driven by plasma-assisted cathodes**
Background gas pressure	~10^{-8} Torr	~10^{-4} Torr
Background gas density	$3 \cdot 10^{8}$ cm^{-3}	$3 \cdot 10^{12}$ cm^{-3}
Background plasma frequency (assuming full ionization)	~10^{8} Hz	~10^{10} Hz
Ratio of plasma frequency to operating frequency	**<10^{-2}**	**<10^{-2}**

As a result, THz MVE sources are much less sensitive to the presence of background plasma than GHz MVE sources. For this reason, THz MVE devices driven by plasma-assisted electron cathodes are projected to be fully compatible with practical vacuum device concepts mandated by the MVE community. In addition, plasma-assisted cathodes are compatible with high pulse repetition rates, and even with continuous wave (CW) operation. They are scalable, can be miniaturized, require neither a filament, nor a filament power-supply, and therefore can be turned on instantly without any warm-up time. They can possibly be gated using simple, low-voltage grids, compatible with moderate vacuum technology and are relatively insensitive to impurities. Finally, no externally applied magnetic field is needed, as an ion channel produced by beam impact ionization of the background gas can be used to guide and transport the beam through the interaction region. For these reasons, plasma-assisted cathodes seem to be attractive candidates to drive vacuum THz sources.

Finally, miniaturized plasma-assisted cathodes could prove to be a breakthrough enabling technology for THz MVE devices, with the potential to advance the technological and scientific base and to impact military, commercial, industrial and scientific applications through the development of transferable, commercially viable technologies. For example, present THz sources are currently notoriously inefficient (1/100 of 1%). With our new approach, there is an exciting opportunity for efficiency enhancement of THz sources by at least two orders of magnitude (or more) because of the extremely high current density and high perveance capabilities of plasma-assisted cathodes.

Most significant accomplishments

The most significant accomplishments are summarized below. (For more details, see Appendix A, and for selected publications see Appendix B.)

Experimental accomplishments

The most significant experimental accomplishment was the demonstration that plasma-assisted miniature cathodes can generate high perveance electron beams at

relatively low voltages (>1000A/cm$^{2;}$ 0.5-3kV), and that those beams could propagate without external guiding magnetic fields over distances compatible with the length of the RF structure of THz sources. This enables the design of future THz sources operating with relatively high efficiency at high power levels.

1) Two types of miniature, plasma-assisted cathodes were designed, fabricated and tested during this research period. Some of the most important characteristics of these guns are summarized in Table 2. Note that very high current densities were successfully demonstrated, ~1000 [A/cm^2], as shown in Table 2 and in Fig. 2.

Table 2: The most important characteristics of plasma-assisted electron guns studied during research period

Beam voltage [kV]	0.5-3
Beam current [A]	0-0.3
Maximum current density [A/cm^2]	~1000

2) Beam propagation over a distance of 10-20 mm was demonstrated in the absence of any external guiding magnetic field. These distances are compatible with the interaction length of THz devices, so this demonstration is very encouraging.

One type of a plasma-assisted cathode was described in a conference article [3]. For more information on both versions of plasma cathodes see Appendix A.

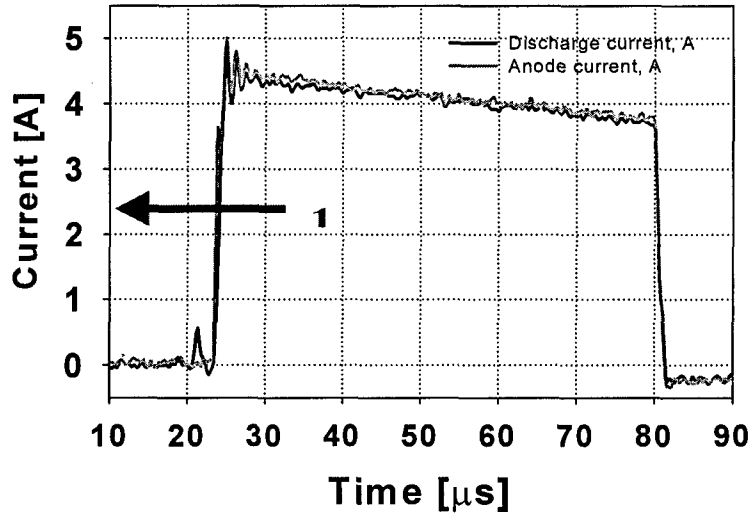

Fig.2. Demonstrated current density as the function of time. Extracted electron current (red) and the plasma discharge current (black) in the glass capillary are almost equal. (For details see Appendix A.)

Theoretical accomplishments

In the framework of the MiPRI program our group had experimentally demonstrated some possibilities to use miniature plasma electron guns for generating electron beams of high current density. In view of these accomplishments, the theoretical efforts were focused on analyzing the possibilities to generate coherent radiation in the THz frequency range with a reasonably high efficiency and at high power levels. Our analysis was restricted by compact devices capable of operation at low voltages. Since at frequencies approaching 1 THz it is much simpler (if not the only possible) to fabricate planar microwave circuits, we considered devices having a planar geometry, which most conveniently can be driven by sheet electron beams. Since high-power operation at very short wavelengths is possible without breakdown only in the case when the interaction space is characterized by dimensions much larger than the wavelength, our analysis was focused on devices using highly selective, oversized resonators (like the orotron whose schematic is shown in Fig. 3).

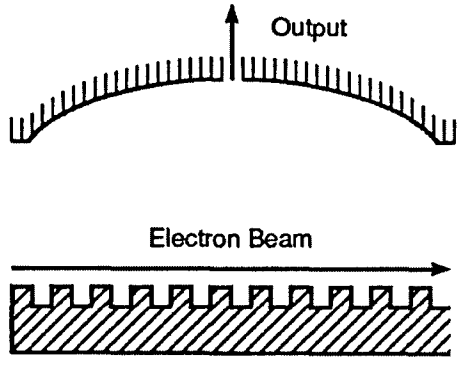

Fig. 3. Schematic of the orotron: an open resonator formed by a concave mirror and a periodic grating plate is excited by a sheet electron beam.

1. The interaction region in the devices specified above has transversely nonuniform interaction space. This nonuniformity should decrease the interaction efficiency. To evaluate the importance of this effect the analytical study had been performed. The analysis performed allowed us to formulate requirements to design

parameters, under which the effect of this nonuniformity on device efficiency is relatively weak. This work was reported [4] and published [5].

2. After a certain analysis it became clear that the device performance is severely limited by the fact that the field of a slow wave moving with the phase velocity close to electron velocity is localized near the slow-wave circuit in a layer whose thickness is much smaller than the wavelength. To position a sheet electron beam within this layer and avoid the beam interception with the circuit requires very fine beam alignment and strong guiding magnetic field. It also requires very high current density for providing in such a narrow electron beam enough current for exciting microwave oscillations in a circuit. To avoid this limitation, two possibilities had been studied.
3. First, we considered the case when the beam current exceeds the start current only slightly that results in excitation of microwave oscillations with small amplitude. In such a case, interaction with the slow wave causes small changes in electron energy. However, this small modulation of electron energies by the RF field can result, at long enough distances, in significant electron bunching improving the device efficiency. Corresponding analytical theory allowing us to make some estimates for optimal operating parameters of the orotron-type devices was developed; results were published [6] and will be presented as an invited keynote at the upcoming 31st Int. Conf. on IR&MM Waves &14th Int. Conf. on THz Electronics, Shanghai, P.R. China [7]. It was found, for example, that in the orotron operating at the frequency of 375 GHz and driven by a 4kV, 0.3 A electron beam having electron current density of 300 A/cm^2 it is possible to produce up to 13 W output radiated power with the efficiency exceeding 1%. Note that such a density can be realized either in non-convergent electron beams generated by cathodes with high current density (such as described above plasma cathodes developed at the University of Maryland) or in convergent electron beams generated by more conventional cathodes with relatively low current density. Also note that a relatively low value of the output efficiency is due to the fact that significant part of the microwave power radiated by an electron beam should be lost due to ohmic losses in the structure walls (the situation typical for so high frequencies).

4. Secondly, we analyzed the case when an electron beam is slightly inclined with respect to the grating plate. The device of such a configuration is known as the clinotron (or "klinotron"). In such a configuration shown in Fig. 4, when the device length is long enough, all electrons of an arbitrarily thick electron beam sooner or later enter the layer occupied by a slow wave near the grating plate. This fact allows one to greatly increase the beam cross-section, mitigate requirements to the electron current density and beam alignment and realize much higher power levels of operation. (Of course, in the case of continuous wave operation some limitations may be imposed by the density of the beam power deposited to the grating plate in the area of beam interception.) The theory describing operation of such devices has been developed recently. The paper describing it is in the process of preparation for publishing in Physics of Plasmas.

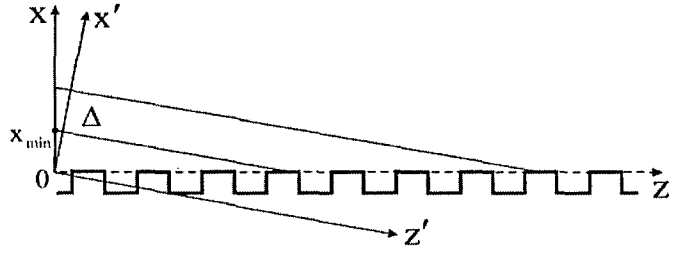

Fig.4. Schematic of the clinotron: a thick electron beam propagates at a small angle with respect to the grating plate and interacts with a slow wave localized near the grating before hitting the plate.

---

[1] www.istok.com

[2] G. Nusinovich, personal communication.

[3] J. Rodgers, R. Chang, V. L. Granatstein, T. M. Antonsen, Jr., G. S. Nusinovich and Y. Carmel "Miniature Plasma Cathode for High-Power Terahertz Sources", The Joint 30th Int. Conf. on IR&MM Waves & 13th Int. Conf. on THz Electronics, Williamsburg, VA, USA, Sept. 19-23, 2005.

[4] G. S. Nusinovich and O. V. Sinitsyn, "Analytical theory of microwave sources with transversely nonuniform interaction space", The Joint 30th Int. Conf. on IR&MM Waves & 13th Int. Conf. on

THz Electronics, Williamsburg, VA, USA, Sept. 19-23, 2005, paper MB4-3, Conf. Digest, pp. 87-88.

[5] G. S. Nusinovich and O. V. Sinitsyn, "Effect of transverse nonuniformity of the rf field on the efficiency of microwave sources driven by linear electron beams", Physics of Plasmas, vol. 12, paper 093107 (September 2005)

[6] G. S. Nusinovich, "Analytical nonlinear theory of the orotron", Physics of Plasmas, vol. 13, paper 053107 (May 2006).

[7] G. S. Nusinovich, "Analytical theory of novel configurations of THz and sub-THz sources driven by linear electron beams" (Invited Keynote), The Joint 31st Int. Conf. on IR&MM Waves &14th Int. Conf. on THz Electronics, Shanghai, P.R. China, Sept. 18-22, 2006.

Appendix A

Two types of plasma-assisted miniature electron guns for THz vacuum devices.

Miniature cathode for THz sources. Electron beam generation and propagation.

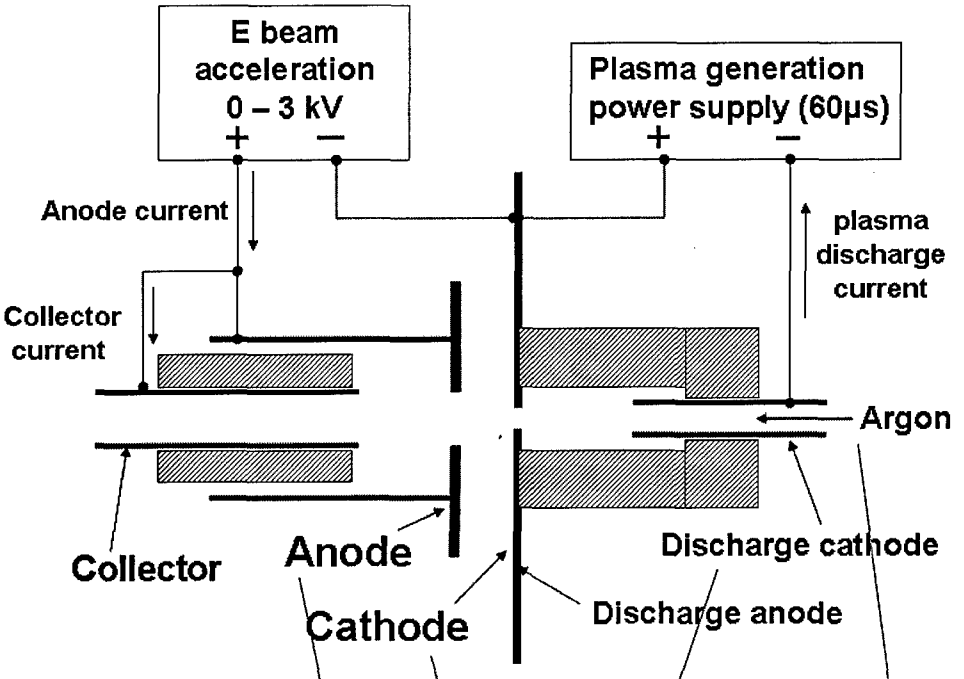

discharge tube 1.4mm ø
discharge tube 6mm long
extraction hole 0.6mmø
anode-cathode gap 1.8mm
anode aperture 1.5mmø
collector aperture 1.2mmø

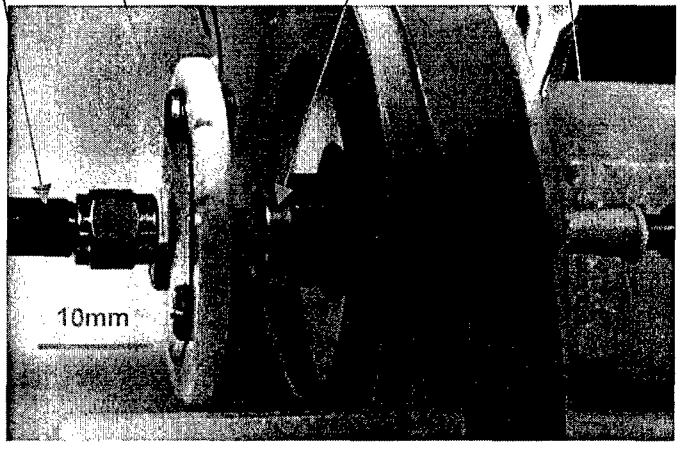

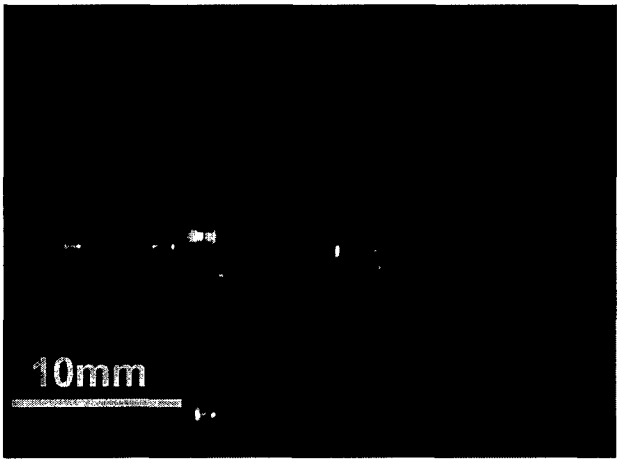

Argon pressure distribution. (Estimated)

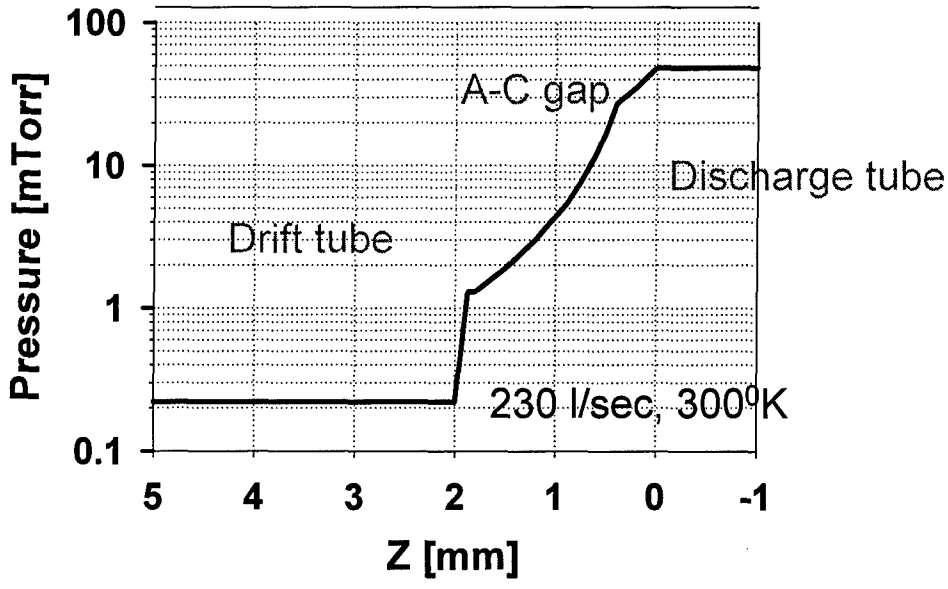

Capilary discharge

Length 6mm,diameter 1.4mm, Pressure 50-500mTorr

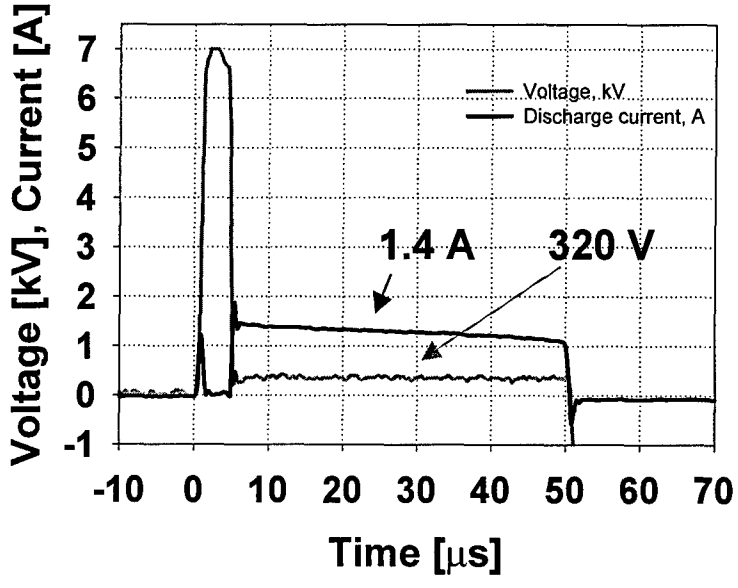

Electron beam extraction and acceleration

Discharge current. Extracted current.

Diameter of extraction = 0.6mm, Voltage=3kV

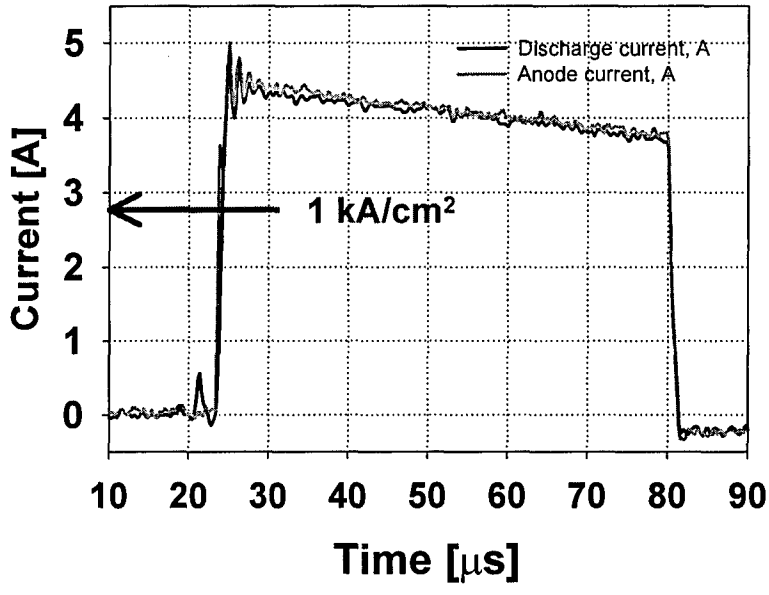

Beam transport / propagation

voltage 3 kV, current 2.7A, pressure 90 mTorr

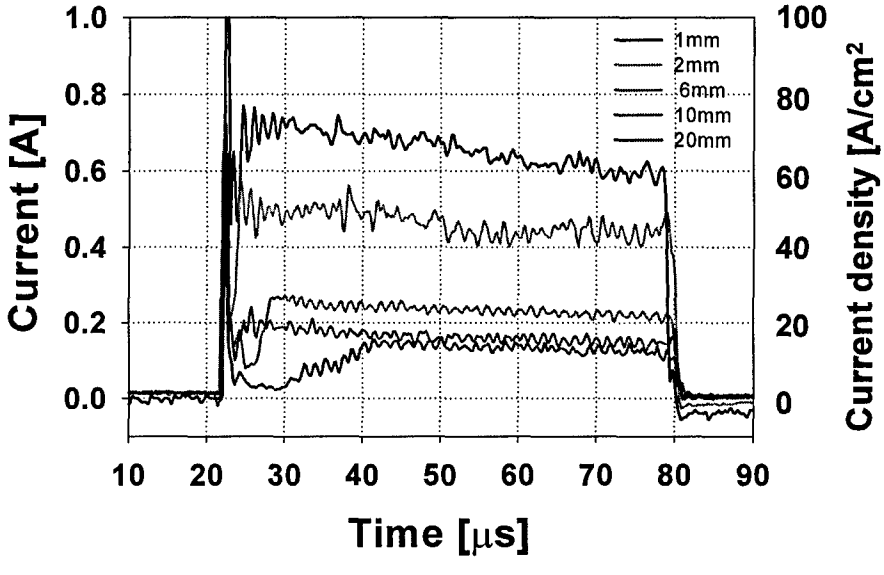

Model of beam transport

Drift tube R=1.8mm, L=30mm, Beam current=1A,
energy=2.8kV,initial radius=0.75mm
Space charge is 100% neutralized

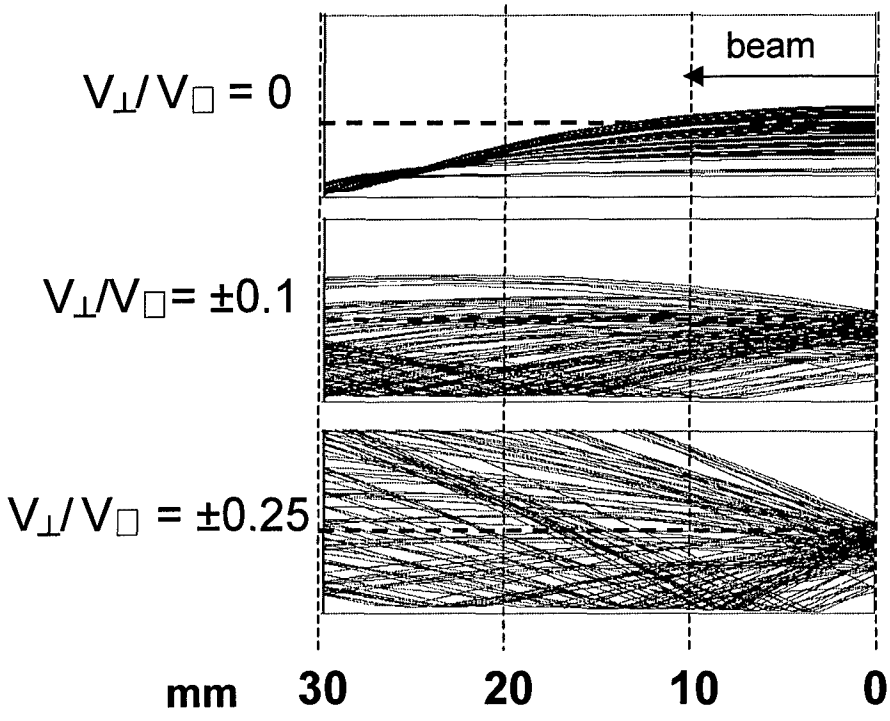

Beam dynamics for different anode currents

3 kV, pressure 50 mTorr

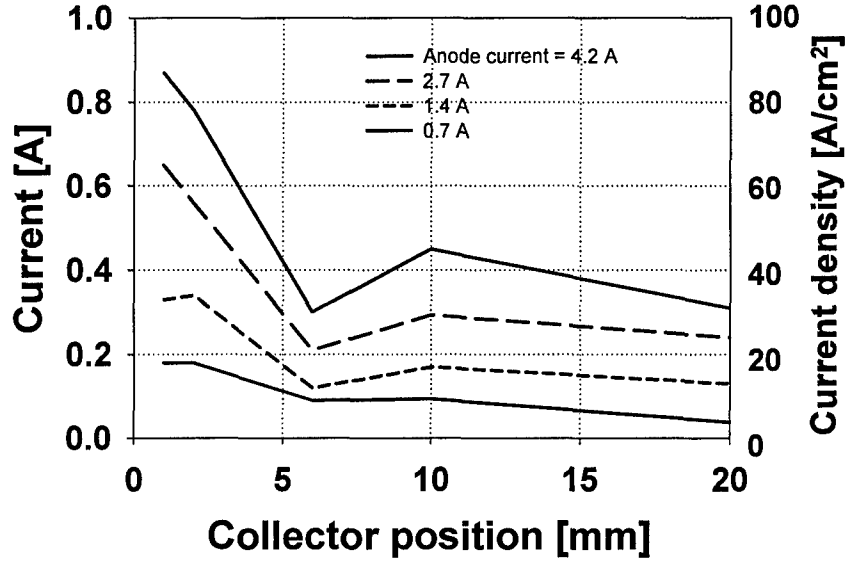

Anode-cathode voltage and current

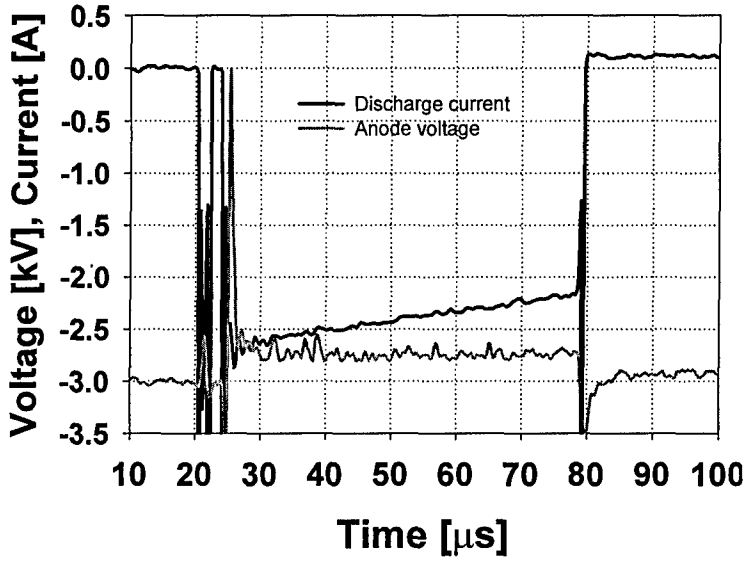

Miniature Plasma Cathode for High-Power Terahertz Sources

J. Rodgers, R. Chang, V. L. Granatstein, T. M. Antonsen, Jr., G. S. Nusinovich and Y. Carmel

Institute for Research in Electronics and Applied Physics
University of Maryland, College Park, MD USA 20742
e-mail: rodgers@umd.edu

Abstract

Efforts to improve efficiency in terahertz vacuum electronic sources such as backward-wave oscillators (BWO) have motivated studies of cathodes capable of generating high-density electron beams so that various interaction circuits may be driven closer to saturation. Preliminary results from experiments on a miniature plasma cathode demonstrate that current densities of up to 1 kA/cm^2 in a 100-micron diameter beam have been achieved. Initial analysis of a 850-GHz, slotted slow-wave structure show that the circuit could be driven at 3-4 times the starting current and that efficiencies of a few percent could be realized. Tests on a gridded plasma cathode show that stable beams of 200 mA at a pulse length of 100 μsec and repetition frequencies of up to 200 Hz were generated.

Introduction

Terahertz sources, such as the clinotron and orotron, are based on Cerenkov emission from the interaction between an electron beam and the electromagnetic field in a slow wave structure (SWS) within an open resonator [1]. However, typical efficiencies even in the most advanced devices are in the 10^{-4} - 10^{-3} range. This is due, in part, because saturated operation is difficult to achieve since devices with thermionic cathodes are limited in terms of current density. Large-area plasma cathodes which were developed for high-power helix BWO's have been demonstrated to reliably generate high current densities (50-500 A/cm^2) [2]. In the present work, increased output power and improved efficiency in terahertz sources will be pursued by developing miniaturized plasma cathodes capable of driving oscillators at several times the starting current. To illustrate, a simple calculation of the starting current in an open-resonator SWS follows.

Calculation of Starting Current

In [3], it was found that the ratio of the amplitude of the synchronous space harmonic of the wave to the amplitude of the zero space harmonic is maximal, when the depth of SWS grooves is equal to a quarter of wavelength and the width of grooves is equal to the half of the structure period. The minimum starting current in the device with a gaussian axial structure of the operating mode can be determined according to [3] as

$$I_{st} = \frac{2\pi^5}{Q_{ohm}} \frac{S_b}{L_{\text{int}}^2} c\beta_0 V_b . \qquad (1)$$

Here S_b is the beam cross-sectional area, L_{int} is the interaction length, β_0 is the velocity of the electrons normalized to the speed of light, c, V_b is the beam voltage and Q_{ohm} is the ohmic quality factor. It has been assumed that total Q is dominated by ohmic losses, which yields the following formula:

$$Q_{ohm} = \frac{H}{\delta_{sk}(3+\lambda/d)}, \qquad (2)$$

where H is the distance between the two mirrors forming the resonator, δ_{sk} is the skin depth, which for copper at 850 GHz is about 0.15 microns, λ is the radiation wavelength and d is the period of the SWS. Note that the ratio of the wavelength to the structure period can be expressed, consistent with the condition of Cherenkov synchronism, in terms of the electron velocity. With H = 2mm, the ohmic Q-factor, depending on the choice of voltage and grating period, is in the range from $1.3 \cdot 10^3$ to $1.7 \cdot 10^3$. Thus the minimum start current density can be determined as

$$j_{st}(A/cm^2) = 2 \cdot 10^4 \frac{\delta_{sk}}{H} \frac{1}{L_{\text{int}}^2(cm)} (1+3\beta_0) V_b(kV) . \qquad (3)$$

It follows from (3) that if the separation between mirrors is 3 mm and the interaction length is 5 mm, the start current density for a 850 GHz clinotron operating 10 kV is equal to 64 A/cm^2. For high efficiency operation the current density should exceed the start current density by at least a factor of 2, which results in the range of nominal current densities of about 130 A/cm^2. For the case of the beam width of 3 mm and beam thickness of 0.1 mm, these numbers correspond to the total beam current of 200-300 mA.

Simple Plasma Cathode

The plasma cathode, which is shown schematically in Fig. 1, was a scaled version of the design given for high-power applications referenced in [2]. The hollow cathode assembly was fabricated from oxygen-free copper with a beam aperture of 1 mm in diameter and a gas port in the back wall in which a 2 mm capillary tube was soldered.

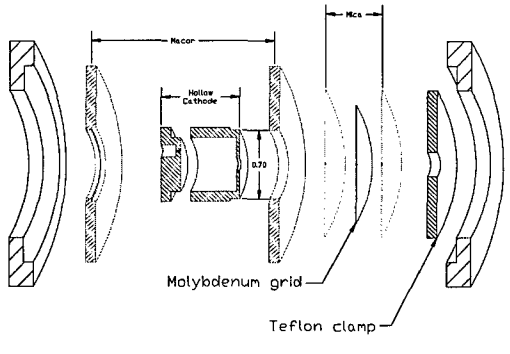

Fig. 1: Expanded cross-sectional diagram of cathode pieces

The grid was fabricated from thin molybdenum sheet and was electrically isolated from the cathode by a mica insulating disk. Both had 100 micron holes for beam extraction that were aligned concentrically with the axis of the hollow cathode during assembly. The assembled gun is shown in Fig. 2 mounted in a vacuum test chamber.

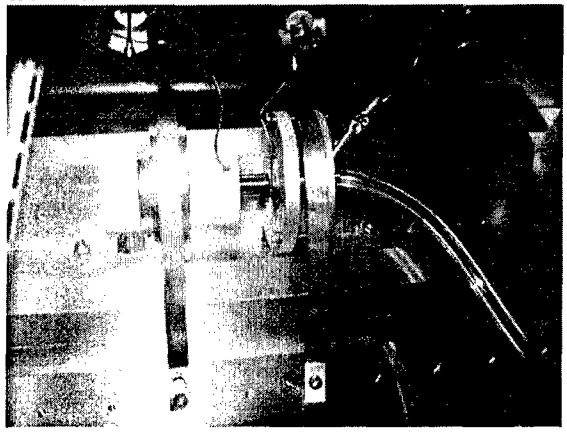

Fig. 2: Miniature plasma cathode shown mounted in a vacuum gun test chamber

The grid was driven by a solid state pulse generator at voltages in the range of 500-800 V, which was determined to be adequate to ionize the fill gas in the hollow cathode in less than 0.5 μsec and pulse lengths in the range 10-200 μsec. The current in the grid-cathode discharge was found to be approximately twice the beam current. The gun was tested according to the parameters given in Table I.

Table I. Experimental Parameters for Gun Test

Beam Voltage	0.5 – 1.1 kV
Beam Current	0 – 0.3 A
Max Current Density	~ 1 kA / cm^2
Plasma Current	0.5 A
Gas (constant source)	N, Ar, Xe
Cathode Pressure	10 - 50 microns
Base Pressure	< 0.01 microns
Pumping	Turbo w/ diff.

A schematic of the test circuit is shown in Fig. 3 along with typical voltage and current waveforms in Fig. 4. The voltage was measured between the cathode and anode giving the total accelerating potential including the DC bias applied between cathode and anode. Figure 5 is a plot of the beam current measured by a wideband current monitor installed around a ground return lead connected to the anode structure. The diameter of the beam was measured to be approximately 70 microns by a witness plate located 2 mm downstream of the extraction aperture.

At this writing, the gun has been operated for periods of up to 12 hours with pulse lengths up to 200 μsec and repetition frequencies up to 100 Hz, corresponding to a maximum duty factor of 2% with only radiation cooling. During the first few minutes of operation, the ionization characteristics of newly fabricated guns drifted somewhat, and the gas pressure had to be decreased to maintain the desired current and voltage. After this short "conditioning" period, the gun characteristics remained stable for many months of operation over a wide range of operating conditions.

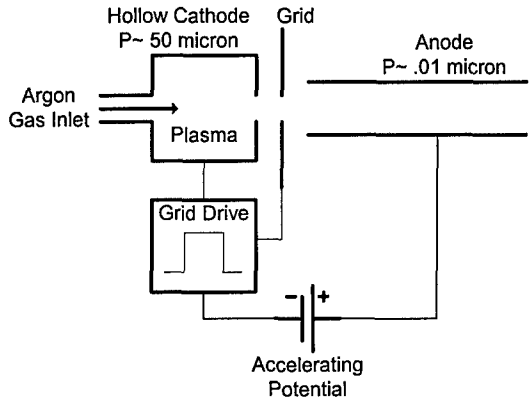

Fig. 3: Schematic of gun test circuit which shows the approximate pressures in the hollow cathode and beam transport regions

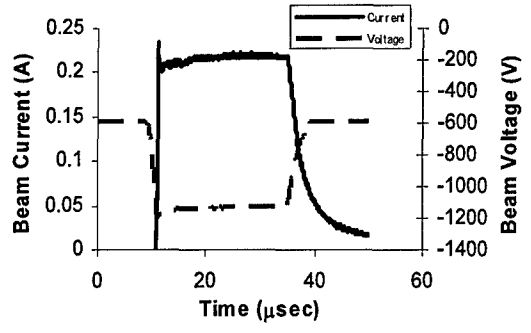

Fig. 4: Typical beam voltage and current traces

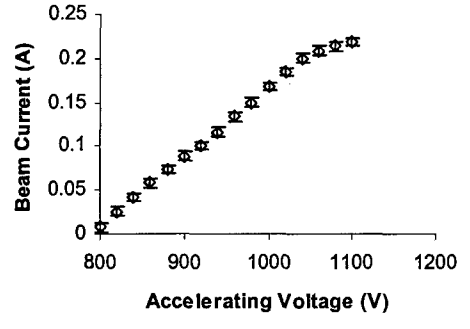

Fig. 5: Measured current-voltage characteristics of plasma gun

References

[1] F. S. Rusin and G. D. Bogomolov, "Oratron," Proc. of the IEEE, vol. 57, 1969, 720-722.

[2] D. M. Goebel et al., "High-power microwave source based on an unmagnetized backward-wave oscillator," IEEE Trans. Plasma Science, vol. 22, 1994, 547-553.

[3] L. A. Weinstein, V. A. Isaev and D. I. Trubetskov, Radiotekhnika I Elektronika, vol. 26, 1983, 1233-1249.

Appendix B: Selected papers

MINIATURE ELECTRON SOURCES FOR TOMORROW'S VACUUM THz DEVICES (MiPRI)

Miniature Plasma Cathode for High-Power Terahertz Sources

J. Rodgers, R. Chang, V. L. Granatstein, T. M. Antonsen, Jr., G. S. Nusinovich and Y. Carmel

Institute for Research in Electronics and Applied Physics
University of Maryland, College Park, MD USA 20742
e-mail: rodgers@umd.edu

Abstract

Efforts to improve efficiency in terahertz vacuum electronic sources such as backward-wave oscillators (BWO) have motivated studies of cathodes capable of generating high-density electron beams so that various interaction circuits may be driven closer to saturation. Preliminary results from experiments on a miniature plasma cathode demonstrate that current densities of up to 1 kA/cm^2 in a 100-micron diameter beam have been achieved. Initial analysis of a 850-GHz, slotted slow-wave structure show that the circuit could be driven at 3-4 times the starting current and that efficiencies of a few percent could be realized. Tests on a gridded plasma cathode show that stable beams of 200 mA at a pulse length of 100 μsec and repetition frequencies of up to 200 Hz were generated.

Introduction

Terahertz sources, such as the clinotron and orotron, are based on Cerenkov emission from the interaction between an electron beam and the electromagnetic field in a slow wave structure (SWS) within an open resonator [1]. However, typical efficiencies even in the most advanced devices are in the 10^{-4} - 10^{-3} range. This is due, in part, because saturated operation is difficult to achieve since devices with thermionic cathodes are limited in terms of current density. Large-area plasma cathodes which were developed for high-power helix BWO's have been demonstrated to reliably generate high current densities (50-500 A/cm^2) [2]. In the present work, increased output power and improved efficiency in terahertz sources will be pursued by developing miniaturized plasma cathodes capable of driving oscillators at several times the starting current. To illustrate, a simple calculation of the starting current in an open-resonator SWS follows.

Calculation of Starting Current

In [3], it was found that the ratio of the amplitude of the synchronous space harmonic of the wave to the amplitude of the zero space harmonic is maximal, when the depth of SWS grooves is equal to a quarter of wavelength and the width of grooves is equal to the half of the structure period. The minimum starting current in the device with a gaussian axial structure of the operating mode can be determined according to [3] as

$$I_{st} = \frac{2\pi^5}{Q_{ohm}} \frac{S_b}{L_{\text{int}}^2} c\beta_0 V_b . \qquad (1)$$

Here S_b is the beam cross-sectional area, L_{int} is the interaction length, β_0 is the velocity of the electrons normalized to the speed of light, c, V_b is the beam voltage and Q_{ohm} is the ohmic quality factor. It has been assumed that total Q is dominated by ohmic losses, which yields the following formula:

$$Q_{ohm} = \frac{H}{\delta_{sk}(3+\lambda/d)}, \qquad (2)$$

where H is the distance between the two mirrors forming the resonator, δ_{sk} is the skin depth, which for copper at 850 GHz is about 0.15 microns, λ is the radiation wavelength and d is the period of the SWS. Note that the ratio of the wavelength to the structure period can be expressed, consistent with the condition of Cherenkov synchronism, in terms of the electron velocity. With H = 2mm, the ohmic Q-factor, depending on the choice of voltage and grating period, is in the range from $1.3 \cdot 10^3$ to $1.7 \cdot 10^3$. Thus the minimum start current density can be determined as

$$j_{st}(A/cm^2) = 2 \cdot 10^4 \frac{\delta_{sk}}{H} \frac{1}{L_{\text{int}}^2(cm)} (1+3\beta_0) V_b(kV) . \qquad (3)$$

It follows from (3) that if the separation between mirrors is 3 mm and the interaction length is 5 mm, the start current density for a 850 GHz clinotron operating 10 kV is equal to 64 A/cm^2. For high efficiency operation the current density should exceed the start current density by at least a factor of 2, which results in the range of nominal current densities of about 130 A/cm^2. For the case of the beam width of 3 mm and beam thickness of 0.1 mm, these numbers correspond to the total beam current of 200-300 mA.

Simple Plasma Cathode

The plasma cathode, which is shown schematically in Fig. 1, was a scaled version of the design given for high-power applications referenced in [2]. The hollow cathode assembly was fabricated from oxygen-free copper with a beam aperture of 1 mm in diameter and a gas port in the back wall in which a 2 mm capillary tube was soldered.

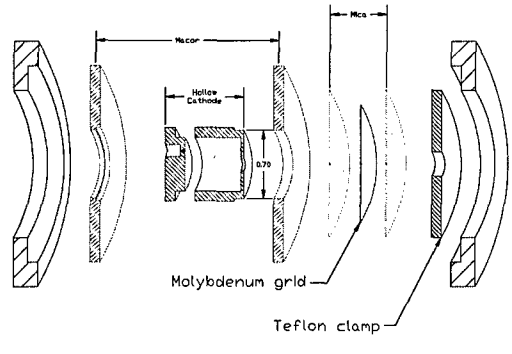

Fig. 1: Expanded cross-sectional diagram of cathode pieces

The grid was fabricated from thin molybdenum sheet and was electrically isolated from the cathode by a mica insulating disk. Both had 100 micron holes for beam extraction that were aligned concentrically with the axis of the hollow cathode during assembly. The assembled gun is shown in Fig. 2 mounted in a vacuum test chamber.

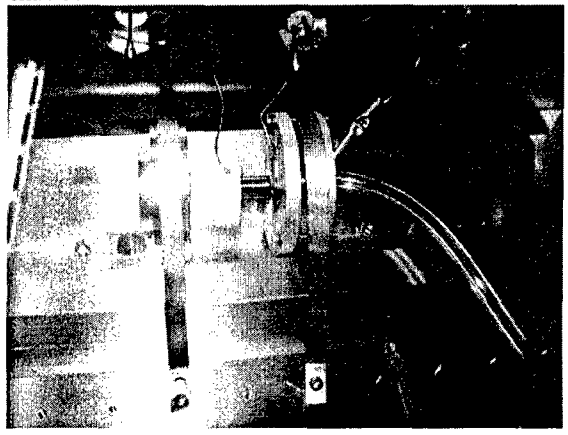

Fig. 2: Miniature plasma cathode shown mounted in a vacuum gun test chamber

The grid was driven by a solid state pulse generator at voltages in the range of 500-800 V, which was determined to be adequate to ionize the fill gas in the hollow cathode in less than 0.5 μsec and pulse lengths in the range 10-200 μsec. The current in the grid-cathode discharge was found to be approximately twice the beam current. The gun was tested according to the parameters given in Table I.

Table I. Experimental Parameters for Gun Test

Beam Voltage	0.5 – 1.1 kV
Beam Current	0 – 0.3 A
Max Current Density	~ 1 kA / cm^2
Plasma Current	0.5 A
Gas (constant source)	N, Ar, Xe
Cathode Pressure	10 - 50 microns
Base Pressure	< 0.01 microns
Pumping	Turbo w/ diff.

A schematic of the test circuit is shown in Fig. 3 along with typical voltage and current waveforms in Fig. 4. The voltage was measured between the cathode and anode giving the total accelerating potential including the DC bias applied between cathode and anode. Figure 5 is a plot of the beam current measured by a wideband current monitor installed around a ground return lead connected to the anode structure. The diameter of the beam was measured to be approximately 70 microns by a witness plate located 2 mm downstream of the extraction aperture.

At this writing, the gun has been operated for periods of up to 12 hours with pulse lengths up to 200 μsec and repetition frequencies up to 100 Hz, corresponding to a maximum duty factor of 2% with only radiation cooling. During the first few minutes of operation, the ionization characteristics of newly fabricated guns drifted somewhat, and the gas pressure had to be decreased to maintain the desired current and voltage. After this short "conditioning" period, the gun characteristics remained stable for many months of operation over a wide range of operating conditions.

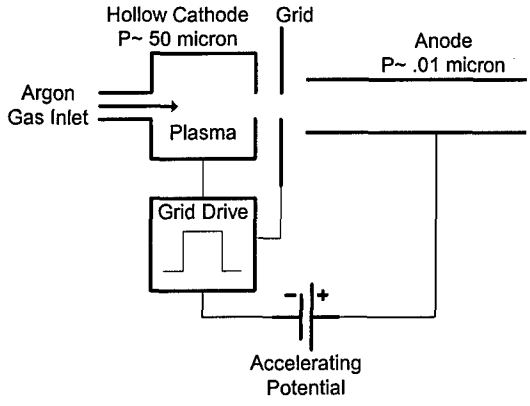

Fig. 3: Schematic of gun test circuit which shows the approximate pressures in the hollow cathode and beam transport regions

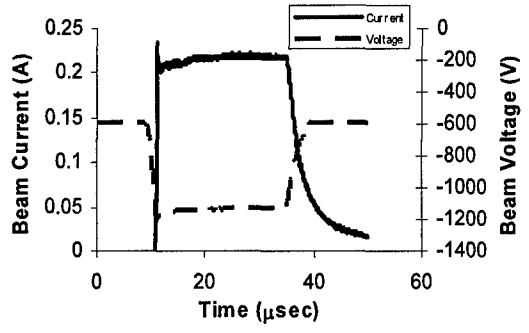

Fig. 4: Typical beam voltage and current traces

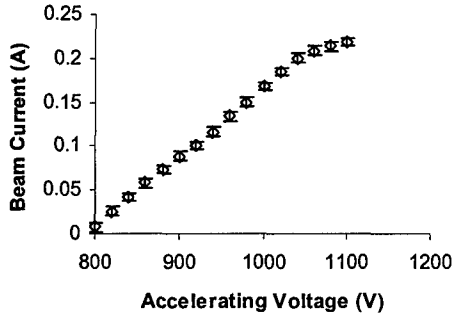

Fig. 5: Measured current-voltage characteristics of plasma gun

References

[1] F. S. Rusin and G. D. Bogomolov, "Oratron," Proc. of the IEEE, vol. 57, 1969, 720-722.

[2] D. M. Goebel et al., "High-power microwave source based on an unmagnetized backward-wave oscillator," IEEE Trans. Plasma Science, vol. 22, 1994, 547-553.

[3] L. A. Weinstein, V. A. Isaev and D. I. Trubetskov, Radiotekhnika I Elektronika, vol. 26, 1983, 1233-1249.

Analytical theory of microwave sources with transversely nonuniform interaction space

G. S. Nusinovich and O. V. Sinitsyn

IREAP, University of Maryland
College Park, MD, USA

IRMMW-THz2005,
Williamsburg, VA,
Sept. 19-23, 2005

INTRODUCTION

Classical microwave vacuum electron devices (klystrons, TWTs, BWOs, magnetrons, gyrotrons) have axially symmetric interaction space.
Therefore, fundamentals of the theory of these devices were developed under assumption about this symmetry.
New demands for escalating performance characteristics as well as novel concepts of microwave sources (e.g., orotrons, sheet-beam klystrons) lead to configurations lacking such a symmetry.
Example: **in the THz range, planar microwave circuits are the most promising.**
To analyze such microwave sources, 2.5D and 3D codes are usually used.

INTRODUCTION (cont.)

2.5D and 3D codes are necessary tools for accurate design of present-day and future microwave sources.
However, before starting these time consuming calculations, it can be useful to have an opportunity to make some simple analytical estimates.

What can be done with the use of a simple analytical theory?

-Analysis of monotron oscillations in sheet-beam klystrons (Nusinovich, Read and Song, Phys. Plasmas, Nov. 2004),
-Analysis of mode coupling in sheet-beam klystrons (Nusinovich, RF-05, Kalamata, Greece, June 2005)
-Analysis of the effect of transverse nonuniformity of the RF field on the efficiency of microwave sources (this presentation)

Formulation of the problem

A beam of electrons moving linearly along the device axis interacts with a synchronous space harmonic of the axial electric field of a resonator.

$$E_z = \mathrm{Re}\left\{ A E_{sz}\left(\vec{r}_\perp\right) f(z) e^{i(\omega t - k_z z)} \right\}$$

$$\frac{d\mathcal{E}}{dt} = -e v_z E_z \qquad \frac{\partial t}{\partial z} = \frac{1}{v_z}$$

For $\gamma = \mathcal{E} / mc^2 = 1/\sqrt{1-\beta^2}$ $\qquad \vartheta = \omega t - k_z z$

$$\frac{\partial \gamma}{\partial z} = -\mathrm{Re}\left\{ A E_{sz} f e^{i\vartheta} \right\} \qquad \frac{\partial \vartheta}{\partial z} = \frac{\gamma}{\sqrt{\gamma^2 - 1}} - h \qquad h = k_z c / \omega$$

The function E_{zs} describes transverse nonuniformity of the RF field acting on electrons

Formulation of the problem (cont.)

Assume that electron density distribution in the device cross-section is described by the function $\Psi\left(\vec{r}_{\perp}\right)$

Then, the interaction efficiency is equal to

$$\eta = \frac{1}{\gamma_0 - 1}\left\{\gamma_0 - \frac{1}{S_b}\int_{S_b}\Psi\left(\vec{r}_{\perp}\right)\left[\frac{1}{2\pi}\int_0^{2\pi}\gamma\left(L\right)d\vartheta_0\right]ds_{\perp}\right\}$$

This is the efficiency of all electron filaments averaged over the cross-section of the interaction space.

What can we do with this general formula?

Quasi-linear approximation

RF amplitude is small and the action of the RF field on streaming electrons is considered as a perturbation.
Equations for e-motion can be solved by the method of successive approximations.
Since odd terms yield zero contribution to the efficiency (due to the averaging over initial phases), to take saturation effects into account one should move up to the 4-th order terms in perturbations of electron energy.

$$\eta = \eta_{lin} - \eta_{sat}$$

Quasi-linear theory (cont.)

$$\eta \propto MC\alpha - M^2 D\beta \qquad M = |A|^2$$

α, β **describe transit effects**

$$C = \frac{1}{S_b}\int_{S_b} \Psi |E_{sz}|^2 \, ds_\perp \qquad D = \frac{1}{S_b}\int_{S_b} \Psi |E_{sz}|^4 \, ds_\perp$$

Maximum efficiency is proportional to $I = \dfrac{C^2}{D}$

This value alone characterizes the effect of transverse nonuniformity of the RF field on the interaction efficiency

EXAMPLES

A. Cylindrical electron beam between two plates	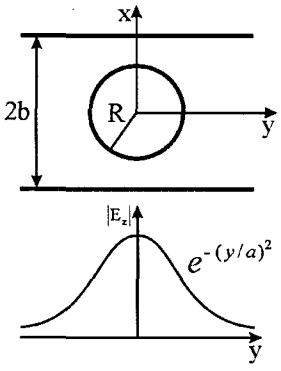
B. Cylindrical electron beam in a rectangular cavity	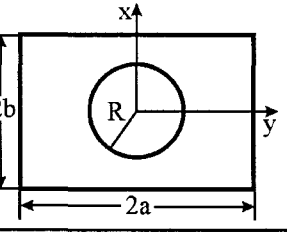
C. Sheet electron beam over the grating plate a) parallel beam - the orotron	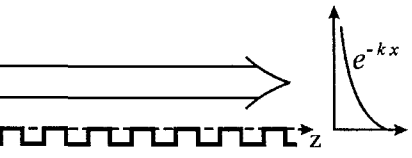
b) inclined beam - the clinotron	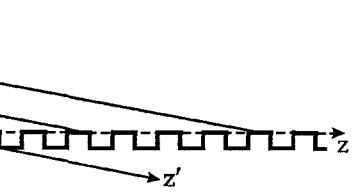

⇐ **As in open Fabry-Perot resonators used in lasers, the RF field profile in the y-direction can be described by Hermite polynomials**

⇐ **Transverse structure is described by sin/cos functions**

⇐ **Exponential decay of the RF field in the x-direction**

RESULTS

Case A

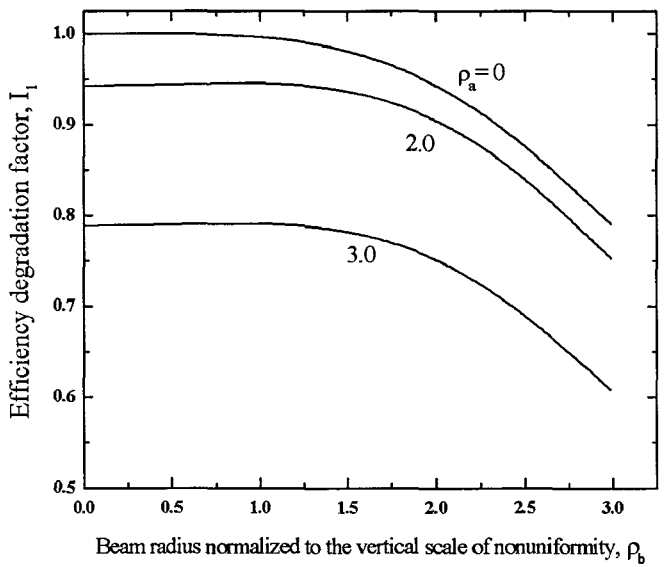

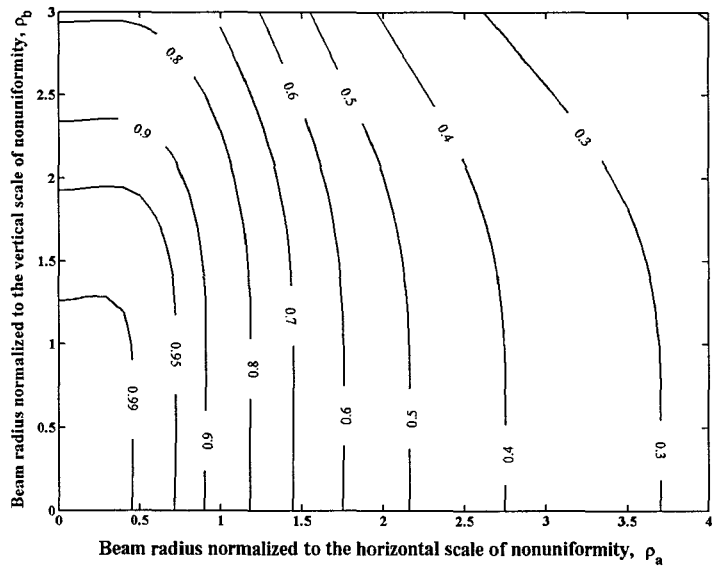

$$\rho_a = R/a$$

$$\rho_b = \pi R/b$$

$$E_z = e^{-(y/a)^2} \cos\left(\frac{\pi}{2}\frac{x}{b}\right)$$

$$R_{\max} = b$$

Maximum value is π

RESULTS (cont.)

Case B
Rectangular cavity

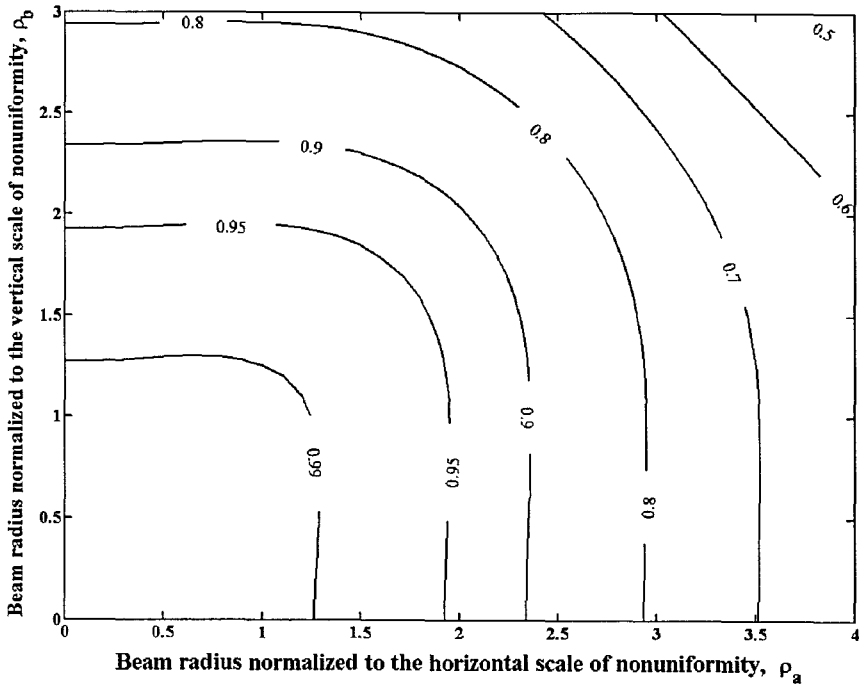

These contours are symmetric with respect to $\rho_b = \rho_a$

$$E_z = \cos\left(m\pi \frac{x}{2b}\right)\cos\left(n\pi \frac{y}{2a}\right) \qquad \rho_a = n\pi R / a \quad \rho_b = m\pi R / b$$

RESULTS (cont.)

Case C(a): the orotron $E_z = A e^{-\kappa x}$

κ **is the absolute value of the transverse wavenumber of the RF field spatial harmonic synchronous with electrons**

The RF field nonuniformity in the wide y-direction is neglected

$$I_3 = \frac{\tanh(\kappa\Delta)}{\kappa\Delta}$$

Δ **is the beam thickness**

The efficiency degrades by a factor of two when the normalized beam thickness $\kappa\Delta$ **is close to 2.0.**

Example: $V_b = 5kV, \lambda = 0.5mm.$

The normalized thickness 2.0 corresponds to the real beam thickness of 0.022mm.

RESULTS (cont.)

Case C(b): the clinotron

Inclination of an electron beam with respect to the surface of a slow-wave structure (grating) allows one to operate with much thicker e-beams, because all electrons sooner or later enter the region of efficient interaction located near the grating surface.
Even a rather small angle of inclination (less than 1 deg) facilitates the device alignment and reduces requirements to the focusing magnetic field.

For the clinotron, the formalism developed above should be modified to take into account the angle between the beam and the grating.

RESULTS (cont.)

$\bar{\alpha} = 0$

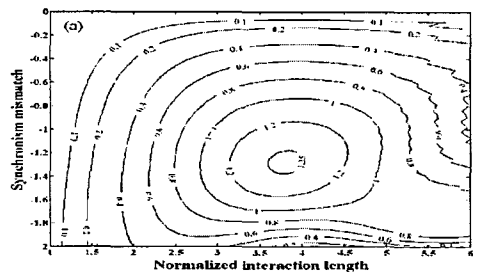

$\bar{\alpha} = 0.1$

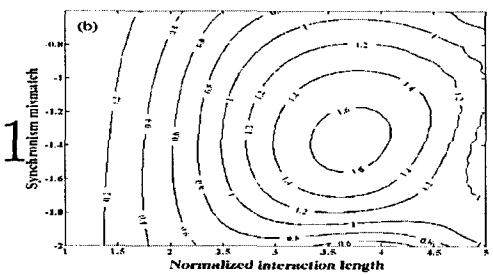

$\bar{\alpha} = 0.2$

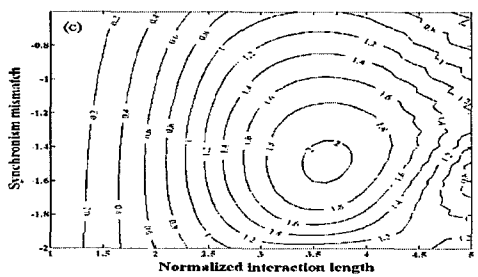

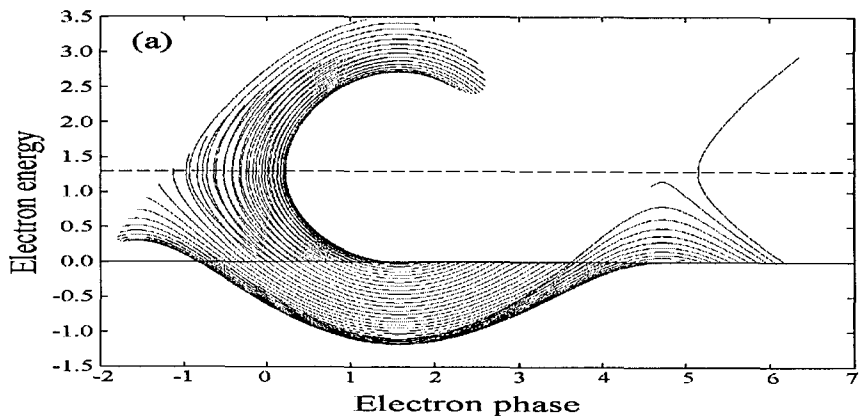

$\bar{\alpha} = 0.1$

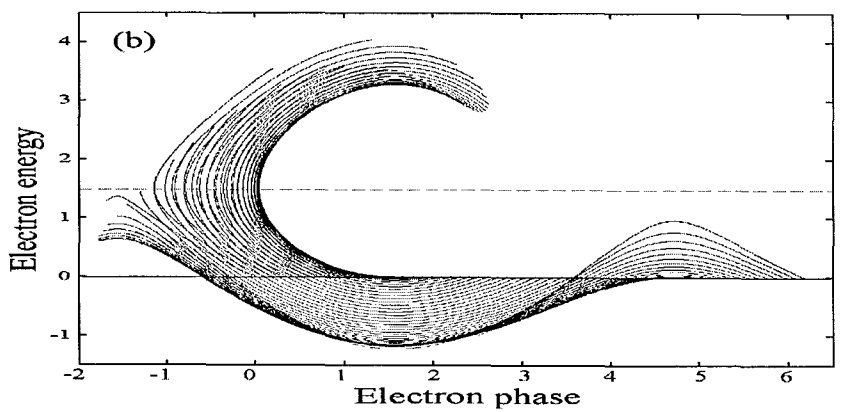

$\bar{\alpha} = 0.2$

$\bar{\alpha}$ **is the inclination parameter**

On the left, contours of the normalized efficiency are shown: $\eta \propto \sqrt{A}\hat{\eta}$

COMPARISON

This simple formalism was applied to the design of a W-band sheet-beam TWT [B. Carlsten et al., IEEE-PS, 85 (2005)] where 1D simulations predicted 24% efficiency, while 2.5D PIC simulations yielded the efficiency close to 22%.

For given beam voltage (120 kV) and beam thickness (0.5 mm) and shape the coefficients C and D defined above are equal to 1.38 and 1.99, respectively.
For the parameter $I=C^2/D$ characterizing the effect of RF field nonuniformity these values of coefficients yield the value close to 0.955.
This value of I reduces the 24% efficiency calculated in 1D simulations to 22.9% that is a little higher than 22% obtained in 2.5D simulations.

Two reasons for this small discrepancy:
-we neglected the RF field nonuniformity in the wide horizontal direction,
- in PIC simulations, near the end of the interaction region, strong pulsations of electrons in the vertical direction were observed, which increase the beam thickness.

SUMMARY

- A simple analytical theory is developed which allows one to easily evaluate the effect of transverse nonuniformity of the RF field on the efficiency of various microwave sources.

2. This issue seems to be especially important for novel sources of THz radiation where the beam thickness can be on the order of or larger than the scale of the transverse nonuniformity of the RF field.
3. This theory can be used for "zero-order" estimates of the efficiency degradation caused by the transverse nonuniformity of the RF field.
4. In principle, any functions describing the beam cross-section and the transverse structure of the RF field (obtained with the use of existing codes) can be substituted into formulas for C and D and, hence, this effect can be easily evaluated.
5. The theory is developed not for competing with code simulations but for complementing them.

NB: for more details see Nusinovich and Sinitsyn, Physics of Plasmas, Paper 093107, Sept. 2005

This work is sponsored by the AFOSR MiPRI program.

Effect of transverse nonuniformity of the rf field on the efficiency of microwave sources driven by linear electron beams

G. S. Nusinovich[a] and O. V. Sinitsyn
Institute for Research in Electronics and Applied Physics, University of Maryland, College Park, Maryland, 20742-3511

(Received 16 May 2005; accepted 22 July 2005; published online 9 September 2005)

This paper contains a simple analytical theory that allows one to evaluate the effect of transverse nonuniformity of the rf field on the interaction efficiency in various microwave sources driven by linear electron beams. The theory is, first, applied to the systems where the beams of cylindrical symmetry interact with rf fields of microwave circuits having Cartesian geometry. Also, various kinds of microwave devices driven by sheet electron beams (orotrons, clinotrons) are considered. The theory can be used for evaluating the efficiency of novel sources of coherent terahertz radiation. © *2005 American Institute of Physics*. [DOI: 10.1063/1.2034427]

I. INTRODUCTION

Many important sources of coherent microwave radiation (such as klystrons, traveling-wave tubes, backward-wave oscillators, magnetrons, and gyrotrons), at least in their simplest configurations, have a cylindrical symmetry of the interaction space. This fact greatly simplifies the theory of such devices and, in many cases, allows developers to do at the first step of design one-dimensional (1D) simulations. Then, some additional factors, such as transverse motion of electrons moving initially linear along the device axis, asymmetry caused by the presence of input and output couplers, etc., can be taken into account.

In many cases, however, new demands for escalating performance characteristics of the existing devices as well as an interest to devices based on new principles of operation lead to analysis of configurations, in which the interaction space does not have an axial symmetry. Orotrons[1,2] as well as sheet-beam[3,4] klystrons can serve as examples of such configurations. As an example of demands resulting in the preference of devices without axial symmetry of the interaction space, one can mention an existing strong interest in the development of sources of coherent terahertz radiation. At so high frequencies it is much simpler (if not the only doable) to fabricate planar microwave circuits (see, e.g., Ref. 5) instead of cylindrical ones.

In such configurations of microwave sources, where electron beams moving initially along the device axis interact with the electromagnetic fields having different amplitude at location of different beamlets, the effect of this transverse nonuniformity on the device efficiency is usually calculated with the use of two-and-one-half-dimensional[6] (2.5D) and three-dimensional[7] (3D) codes. For initial evaluation of the effect of this nonuniformity on the device efficiency, however, some analytical methods can be proposed. These methods should be treated as complementary to 3D code simulations. The purpose of such methods is to help designers to easily evaluate the effect of transverse nonuniformity of the rf field on the device efficiency before starting some time-consuming 3D simulations.

In this paper, we propose some of such methods and give some estimates of the effect of transverse nonuniformity on the efficiency in several device configurations. The paper is organized as follows. In Sec. II, the formalism describing the quasilinear theory is presented. Such a theory was originally used for evaluating the effect of transverse nonuniformity of the rf field on the efficiency of the gyrotron.[8] In Sec. III, a number of examples are considered that illustrate the application of the method to some specific configurations. In Sec. IV, a simple nonlinear theory describing similar effects in the clinotron[9] is developed. In Sec. V we apply the developed formalism to the design of a W-band traveling-wave tube (TWT), which was done with the use of 1D and 2.5D simulations,[10] and compare the results of our analytical treatment with the data of numerical simulations. Finally, Sec. VI contains a brief discussion and summary.

II. QUASILINEAR THEORY

A. General formalism

Let us consider a beam of electrons moving linearly along the device axis with the velocity v_z and interacting with a synchronous space harmonic of the axial electric field of a resonator,

$$E_z = \mathrm{Re}\{AE_{sz}(\mathbf{r}_\perp)f(z)e^{i(\omega t - k_z z)}\}. \tag{1}$$

Here the functions $f(z)$ and $E_{sz}(\mathbf{r}_\perp)$ describe the axial and transverse structures of this field, respectively.

Electron motion in such a 1D case can be described by equations for the electron energy ε and time that a particle spends in the interaction space:

$$\frac{d\varepsilon}{dt} = -ev_z E_z, \tag{2}$$

[a]Author to whom correspondence should be addressed; electronic mail: gregoryn@umd.edu

$$\frac{\partial t}{\partial z} = \frac{1}{v_z}. \tag{3}$$

Below we will consider a stationary electron beam, for which in (2) $d/dt=\partial/\partial t+v_z(\partial/\partial z)=v_z(\partial/\partial z)$. Hence, introducing a slowly variable phase difference between electrons and the phase of the synchronous wave, $\vartheta=\omega t-k_z z$, and normalized variables $z'=(\omega/c)z$, $\gamma=\varepsilon/mc^2$, $\beta=v_z/c$, $h=k_z c/\omega$, and $A'=eA/mc\omega$, we can rewrite (2) and (3) omitting primes as

$$\frac{\partial\gamma}{\partial z} = -\mathrm{Re}\{AE_{sz} f e^{i\vartheta}\}, \tag{4}$$

$$\frac{\partial\vartheta}{\partial z} = \frac{\gamma}{\sqrt{\gamma^2-1}} - h. \tag{5}$$

In (5), the general relation between electron energy and velocity, $\gamma=1/\sqrt{1-\beta^2}$, was used. Equations (4) and (5) should be supplemented by the initial conditions: $\gamma(0)=\gamma_0$ and $\vartheta(0)=\vartheta_0$, where the entrance phase ϑ_0 is uniformly distributed from 0 to 2π. Below we will assume that the beam is monoenergetic, i.e., the spread in the initial energies is negligibly small.

Transverse nonuniformity of the rf field, which was discussed in the Introduction, is described in Eq. (4) by the function $E_{sz}(\mathbf{r}_\perp)$. Correspondingly, the efficiency of a beam, whose density distribution in the device cross section can be given by the function $\Psi(\mathbf{r}_\perp)$, can be determined as

$$\eta = \frac{1}{\gamma_0-1}\left\{\gamma_0 - \frac{1}{S_b}\int_{S_\perp}\Psi(\mathbf{r}_\perp) \times\left[\frac{1}{2\pi}\int_0^{2\pi}\gamma(L)d\vartheta_0\right]ds_\perp\right\}. \tag{6}$$

Note that the function $\Psi(\mathbf{r}_\perp)$ obeys the normalization condition $\int_{S_b}\Psi(\mathbf{r}_\perp)ds_\perp=S_b$, where S_b is the cross-sectional area of the beam. Also in (6) $L=\omega L/c$ is the normalized length of the interaction space.

B. Quasilinear approximation

In the framework of a quasilinear theory, we will consider the effect of the rf field on electron motion by a method of successive approximations assuming the amplitude of the rf field, A, in Eqs. (4) and (5) to be a small parameter. Note that this assumption, as follows from normalization of the amplitude, corresponds to the restriction on the original amplitude of the rf field $A(\mathrm{kV/cm})\ll 2\pi\cdot 511/\lambda(\mathrm{cm})$, which is practically always fulfilled. The first steps in this derivation are quite similar to those described in Ref. 11.

In the zero-order approximation, electron energy and phase are equal to

$$\gamma_{(0)}=\gamma_0, \quad \vartheta_{(0)}=\vartheta_0+\delta z. \tag{7}$$

Here we introduced initial mismatch of synchronism between electrons and the wave, $\delta=1/\beta_0-h$.

First-order terms in electron motion follow from representations $\gamma=\gamma_{(0)}-\gamma_{(1)}$ and $\vartheta=\vartheta_{(0)}+\vartheta_{(1)}$, in which the last terms at right-hand sides proportional to A are much smaller than the first ones. These perturbations in electron motion, as follows from (4) and (5), are equal to

$$\gamma_{(1)}=\mathrm{Re}\{e^{i\vartheta_0}AE_{sz}u\}, \tag{8}$$

$$\vartheta_{(1)}=\frac{1}{(\gamma_0^2-1)^{3/2}}\mathrm{Re}\{e^{i\vartheta_0}AE_{sz}v\}. \tag{9}$$

Here we introduced $u=\int_0^z f e^{i\delta z'}dz'$ and $v=\int_0^z u(z')dz'$. First-order perturbations in electron energy, being substituted in the formula for the device efficiency (6), yield zero after averaging over the entrance phases. Therefore, even for obtaining the region of parameters where the self-excitation of the device is possible, it is necessary to calculate the second-order terms, i.e., $\gamma_{(2)}$ proportional to A^2, as it was done in Ref. 11. Representing the electron energy as $\gamma=\gamma_{(0)}-\gamma_{(1)}-\gamma_{(2)}$ and linearizing the right-hand side of Eq. (4) up to the second-order terms, one can readily obtain the solution for $\gamma_{(2)}$:

$$\gamma_{(2)}=\mathrm{Re}\left\{iAE_{sz}e^{i\vartheta_0}\int_0^z f(z')e^{i\delta z'}\vartheta_{(1)}(z')dz'\right\}.$$

To calculate the efficiency, one should average this change in energy over the entrance phases and transverse coordinates of beamlets. Resulting expression for the efficiency valid in the framework of the linear theory is the following:

$$\eta_{\mathrm{lin}}=|A|^2\frac{1}{2(\gamma_0-1)(\gamma_0^2-1)^{3/2}}C\,\mathrm{Re}\,\mathcal{F}_{\mathrm{lin}}. \tag{10}$$

Here

$$C=\frac{1}{S_b}\int_{S_b}\Psi(\mathbf{r}_\perp)|E_{sz}(\mathbf{r}_\perp)|^2ds_\perp \tag{11}$$

is the coefficient describing the coupling of an electron beam to the synchronous component of the rf field and $\mathrm{Re}\,\mathcal{F}_{\mathrm{lin}}$ is the real part of

$$\mathcal{F}_{\mathrm{lin}}=-i\int_0^L f^*(z)e^{-i\delta z}v(z)dz, \tag{12}$$

which is the complex "linear" gain function equivalent to the beam-loading conductance known in the theory of klystrons (see, e.g., Ref. 12).

Next, we shall calculate the saturation terms in the dependence of the efficiency on the rf field amplitude. For doing this, it is necessary to move with the method of successive iterations further up to the fourth-order term in electron energy, because the third-order terms yield zero after averaging over the entrance phase, as it happened with the first-order terms considered above. Omitting the details of rather lengthy derivation, we will give here the final expression for the saturation terms in the efficiency, which in the framework of the quasilinear theory can be presented as

$$\eta=\eta_{\mathrm{lin}}-\eta_{\mathrm{sat}}. \tag{13}$$

For a device with long enough interaction length ($L=\omega L/c \gg 1$), this saturation term η_{sat} is equal to

$$\eta_{\text{sat}} = |A|^4 \frac{1}{8(\gamma_0 - 1)(\gamma_0^2 - 1)^{9/2}} D \operatorname{Re} \mathcal{F}_{\text{sat}}. \tag{14}$$

Here the coefficient

$$D = \frac{1}{S_b} \int_{S_b} \Psi(\mathbf{r}_\perp) |E_{sz}(\mathbf{r}_\perp)|^4 ds_\perp \tag{15}$$

describes the effect of transverse nonuniformity of the rf field on the saturation, and Re $\mathcal{F}_{\text{sat}}$ is the real part of the gain function describing the saturation in the framework of the quasilinear theory:

$$\mathcal{F}_{\text{sat}} = -i \int_0^L f^* e^{-i\delta z} \left[\int_0^z \left(2u^* \int_0^{z'} \int_0^{z''} u^2 dz''' dz'' - \int_0^{z'} u^2 v^* dz'' + u^* v^2 \right) dz' \right] dz. \tag{16}$$

Note that this formula (16) coincides with the definition of the self-saturation coefficient derived in the theory of mode interaction in gyrotrons.[13]

Substituting all these expressions into (13) results in the following formula for the efficiency in the quasilinear approximation:

$$\eta = \frac{1}{2(\gamma_0 - 1)(\gamma_0^2 - 1)^{3/2}} \left\{ |A|^2 C \mathcal{F}'_{\text{lin}} - \frac{1}{4(\gamma_0^2 - 1)^3} |A|^4 D \mathcal{F}'_{\text{sat}} \right\}. \tag{17}$$

Here the primes denote the real parts of the gain functions, and the coefficients C and D determined above characterize the effect of the transverse nonuniformity of the rf field on the device efficiency in the small-signal regime and in the saturation stage, respectively. From (17) one can easily find the optimal intensity of the rf field, $M = |A|^2$:

$$M_{\text{opt}} = 2(\gamma_0^2 - 1)^3 \frac{\mathcal{F}'_{\text{lin}}}{\mathcal{F}'_{\text{sat}}} \frac{C}{D}. \tag{18}$$

Maximum efficiency that corresponds to this intensity is equal to

$$\eta_{\max} = \frac{(\gamma_0^2 - 1)^{3/2}}{2(\gamma_0 - 1)} \frac{(\mathcal{F}'_{\text{lin}})^2}{\mathcal{F}'_{\text{sat}}} \frac{C^2}{D}. \tag{19}$$

At low voltages, the first term at the right-hand side of (19) can be reduced to $(\gamma_0^2 - 1)^{3/2}/2(\gamma_0 - 1) \simeq [2(eV_b/mc^2)]^{1/2}$. As follows from (19), the effect of the transverse nonuniformity of the rf field on the device maximum efficiency can be estimated by the ratio

$$I = \frac{C^2}{D} = \frac{\left[(1/S_b) \int_{S_b} \Psi |E_{sz}|^2 ds_\perp \right]^2}{(1/S_b) \int_{S_b} \Psi |E_{sz}|^4 ds_\perp}. \tag{20}$$

So, the maximum efficiency depends on the difference between the effects of transverse nonuniformity on the linear and nonlinear properties of an oscillator, which are described by the coefficients C and D, respectively. The application of this formula to various specific configurations of microwave circuits and electron-beam cross sections is given in Sec. III.

TABLE I. Typical configurations of microwave sources with transversely nonuniform interaction space.

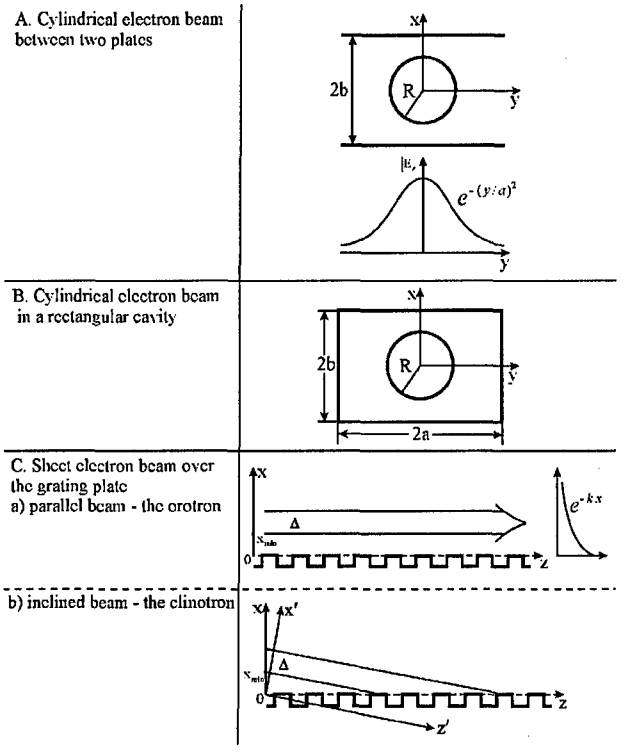

III. EXAMPLES

In this and next sections we will study the effect of the transverse nonuniformity of the rf field in the device configurations that are schematically shown in Table I. The first one is a cylindrical pencil-like electron beam inserted in the rf structure formed by two parallel plates. (Such a structure can model the cavities used in sheet-beam klystrons.) The second example is the same beam inserted in a rectangular cavity. The third example is a sheet electron beam propagating over the surface of grating plate. The case of parallel propagation of this beam, which models the interaction in the orotron,[1,2] will be considered in this section. The case of a tilted beam, which models the clinotron[9,14] and needs a certain modification of the theory, will be considered in Sec. IV.

A. Cylindrical beam between two parallel plates

As well as in open Fabry-Perot resonators used in lasers, the rf field in the wide transverse (y) dimension can be described by Hermite polynomials. Below we will restrict our consideration by the lowest-order Hermite polynomial, which is the Gaussian profile, because the modes with a larger number of variations in y direction have higher diffraction losses through the open ends. The field distribution between the plates, i.e., in x direction, can be represented as a standing-wave pattern. Below we will consider a mode

with one variation in this direction, because modes with a larger number of such variations have much higher frequencies. Thus, the dependence of the axial component of the electric field will be given as

$$E_z = e^{-(y/a)^2} \cos\left(\frac{\pi}{2}\frac{x}{b}\right), \tag{21}$$

where the parameters a and b characterize the scale of the rf field nonuniformity in y and x directions, respectively, and x varies from $-b$ to b between the plates. Regarding an electron beam we assume that this is a cylindrical solid beam of a radius R.

Substituting (21) and the beam coordinates into (11) and (15) yields the following expressions for the coefficients C and D, respectively:

$$C = \frac{2}{\pi}\int_0^1 e^{-2\rho_a^2 v^2}\left\{\sqrt{1-v^2} + \frac{1}{\rho_b}\sin(\rho_b\sqrt{1-v^2})\right\}dv, \tag{22}$$

$$D = \frac{1}{2\pi}\int_0^1 e^{-4\rho_a^2 v^2}\left\{3\sqrt{1-v^2} + \frac{4}{\rho_b}\sin(\rho_b\sqrt{1-v^2}) + \frac{1}{2\rho_b}\sin(2\rho_b\sqrt{1-v^2})\right\}dv. \tag{23}$$

In (22) and (23), we introduced normalized variables and parameters: $v=y/R$, $\rho_a=R/a$, and $\rho_b=\pi R/b$. Then, expressions given by (22) and (23) were substituted into Eq. (20).

The results of the calculations are shown in Fig. 1. Here Fig. 1(a) shows the dependence of the factor I_1, which characterizes the effect of the transverse nonuniformity on the device efficiency for our model, on the parameter ρ_b for several values of ρ_a, and Fig. 1(b) shows the contours of equal values of I_1 in the plane of parameters ρ_b vs ρ_a. Note that the maximum value $\rho_{b,\max}=\pi$ corresponds to the beam diameter equal to the distance between the plates. (Let us call the readers' attention to the difference in notations for ρ_a and ρ_b by a factor of π.) As follows from these data, as far as the beam radius does not exceed $2a$, which is the width of the Gaussian distribution at the e^{-1} level, and also is not larger than one-third of the distance between the plates, the efficiency decreases by less than a factor of 2.

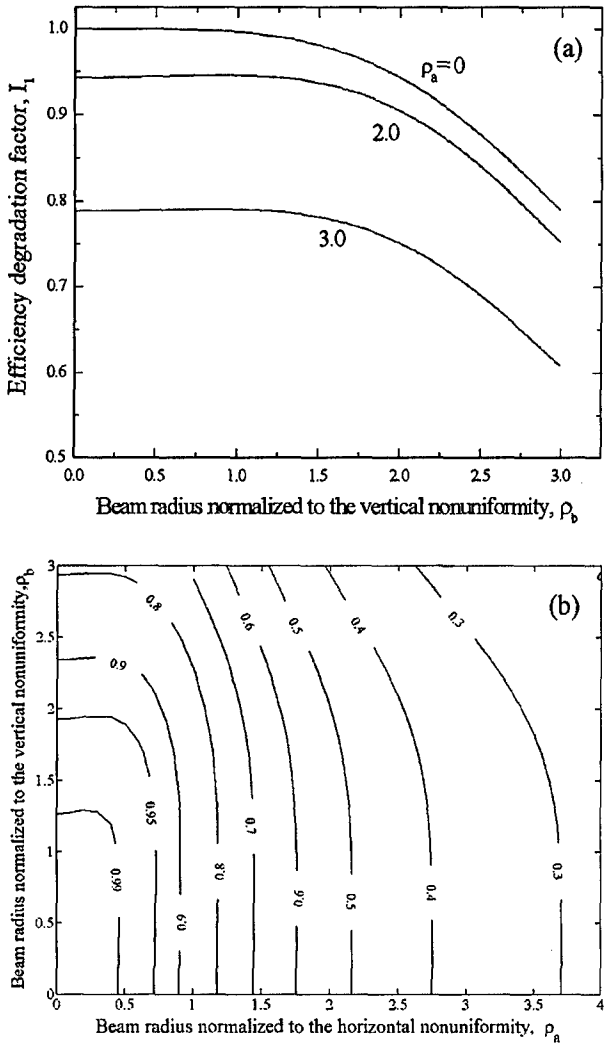

FIG. 1. Effect of nonuniformity on the interaction efficiency of a cylindrical electron beam located between two parallel plates: (a) the factor I_1 as the function of the parameter ρ_b characterizing the field nonuniformity between two plates for several values of the parameter ρ_a characterizing the field variation in a wide transverse direction; (b) contours of constant values of I_1 in the plane of parameters ρ_b vs ρ_a.

B. Cylindrical beam in a rectangular cavity

The axial component of the rf electric field in a rectangular cavity for the case of odd number of field variations in transverse dimensions can be given as

$$E_z = \cos\left(m\pi\frac{x}{2b}\right)\cos\left(n\pi\frac{y}{2a}\right). \tag{24}$$

(In the case of even m or n cos should be replaced by sin.) Note that Eq. (24) is written for the reference frame with the origin in the center of a cavity.

Assuming that the beam center coincides with this origin, one can substitute (24) into (11) and (15) and using a given geometry of a pencil-like beam readily arrive at the following expressions for coefficients C and D:

$$C = \frac{1}{4} + \frac{1}{2\rho_a}J_1(\rho_a) + \frac{1}{2\rho_b}J_1(\rho_b) + \frac{1}{\pi\rho_b}\int_0^1 \cos(\rho_a v)\sin(\rho_b\sqrt{1-v^2})dv, \tag{25}$$

$$D = \frac{1}{16\pi}\int_0^1 [\cos(2\rho_a v) + 4\cos(\rho_a v) + 3]\times\left\{3\sqrt{1-v^2} + \frac{4}{\rho_b}\sin(\rho_b\sqrt{1-v^2}) + \frac{1}{2\rho_b}\sin(2\rho_b\sqrt{1-v^2})\right\}dv. \tag{26}$$

Here $\rho_a=n\pi R/a$ and $\rho_b=m\pi R/b$. In (25) we used the known integral (see, e.g., 3.752.2 in Ref. 15): $\int_0^1\sqrt{1-v^2}\cos(\rho v)dv = (\pi/2\rho)J_1(\rho)$.

Substituting these formulas for C and D into Eq. (20) readily yields the value of the ratio I_2 characterizing the effect of transverse nonuniformity on the efficiency. Contours

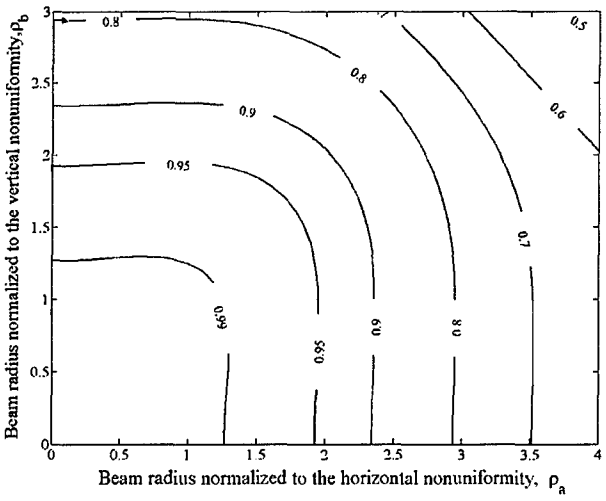

FIG. 2. Effect of nonuniformity of the interaction efficiency of a cylindrical electron beam in a rectangular cavity: contours of constant values of the factor I_2 are shown in the plane of parameters characterizing the field nonuniformity in both transverse directions.

of I_2=const are shown in Fig. 2 in the plane ρ_b vs ρ_a. Of course, these contours are symmetric with respect to $\rho_b=\rho_a$. Recall that for modes with one variation the maximum value of a corresponding parameter ρ does not exceed π. Within $\rho_{a,b}\leqslant\pi$ the factor I_2 is larger than 0.7, i.e., efficiency degradation is not very strong. Note that the dependence of I_2 on the parameter ρ_b is essentially the same as the dependence of I_1 shown in Fig. 1 because this normalized variable ρ_b has the same meaning in both cases. At the same time, the ratio I_2 is less sensitive to the variable ρ_a than the ratio I_1 because of the difference in normalization of the beam radius in this variable to the horizontal scale of the rf field nonuniformity in both cases. For instance, if we assume that the scale of horizontal nonuniformity, $a^{(A)}$, of the Gaussian distribution in case A is equal to the distance between sidewalls, $a^{(B)}$, in case B and the rf field in the latter case has only one variation in y direction, we get the following relation between variables ρ_a for both cases: $\rho_a^{(B)}=\pi\rho_a^{(A)}$. So, in this specific example the values of I_2 shown in Fig. 2 for, let say, $\rho_a=\pi$ should be compared with the values of I_1 shown in Fig. 1(b) for $\rho_a=1$. Of course, this coefficient of proportionality depends on the position of sidewalls in case B.

C. The orotron

In microwave sources based on the use of coherent Cherenkov radiation, electrons interact with a synchronous electromagnetic wave (or synchronous space harmonic of it in a periodic slow-wave structure), which propagates in the direction of electron flow with the phase velocity, $v_{ph}=\omega/k_z$, smaller than the speed of light c. Correspondingly, the axial wave number k_z of such of a wave is larger than ω/c and, hence, such a wave has an imaginary transverse wave number, which characterizes the decay of this wave with the distance from the surface of a slow-wave structure. As follows from the condition of Cherenkov synchronism between this slow wave and electrons, the size of the region of transverse localization of such a slow wave can be estimated as (see, e.g., Ref. 16) $L_\perp\sim(\gamma_0^2-1)^{1/2}\lambda$. At low voltages, where $(\gamma_0^2-1)^{1/2}\approx(2eV_b/mc^2)^{1/2}\ll 1$, and at short wavelengths, this distance is very small. Therefore the effect of the finite thickness of an electron beam becomes well pronounced.

To estimate the role of this effect on the interaction efficiency, consider a simple model, in which only the effect of the transverse exponential decay of the rf field of a slow wave is taken into account. Such a model is shown in Table I. First, consider the case of the orotron where an electron beam propagates parallel to the grating plate.

Let us represent the axial rf electric field as

$$E_z=Ae^{-\kappa x}, \tag{27}$$

where κ is the absolute value of the wave number in the x direction. Assume that a sheet electron beam has a finite thickness Δ and its midplane is located at the distance $x^*=x_{\min}+\Delta/2$, where $x_{\min}$ is the clearance between the beam and the grating surface. Edge effects in the y direction will be neglected. Consider the case when the rf field amplitude is optimal for electrons located in the midplane. Then, with the use of (27) one can readily get the following simple formula for the factor I:

$$I_3=\frac{\tanh(\kappa\Delta)}{\kappa\Delta}. \tag{28}$$

As follows from (28), the efficiency degrades by a factor of 2 when the normalized thickness $\kappa\Delta$ is close to 2.0. For instance, in a device driven by a 5-kV electron beam and operating at a 0.5-mm wavelength, this normalized thickness of 2.0 corresponds to the real beam thickness of 0.022 mm.

IV. THE CLINOTRON

As is known, to mitigate the issue associated with efficiency and power degradation at short wavelengths caused by miniaturization of the interaction space and corresponding clearance between the beam and the grating plate, the device called the clinotron was proposed.[9] The key distinction between the clinotron and other slow-wave devices (such as backward-wave oscillators and orotrons) is an inclined position of an electron beam with respect to the surface of a slow-wave structure. In such a device, even electrons of a relatively thick beam can sooner or later interact with a strong enough rf field near the grating surface. As shown in Ref. 9 (see also Ref. 14 for latest references), even a rather small angle of inclination (less than 1 deg) allows one to greatly increase the radiated microwave power and facilitates the device alignment and the requirements to the focusing magnetic field. It should be noted that, according to Ref. 9, first papers on the theory and experiments with clinotrons were published in USSR in 1958, while in 1957 Karp published his paper on the experiments with backward-wave oscillators (BWOs),[17] in which the principle of the clinotron and corresponding improvements in the BWO performance in the case of a tilted electron beam were described.

To apply our formalism to the clinotron, introduce the reference frame associated with a beam inclined at the angle α where the axial z' and transverse x' coordinates are related to the coordinates z and x used above as:

$$z' = z\cos\alpha - x\sin\alpha, \quad x' = z\sin\alpha + x\cos\alpha. \tag{29}$$

At small angles α, the most important effect is the dependence of the exponential term of the rf field acting upon electrons in (27) on z': $E_z = Ae^{-\kappa x} = Ae^{-\kappa(x_0-\alpha z')}$. Here x_0 is the transverse coordinate of an electron at the entrance.

Let us now modify the basic Eqs. (4)–(6) for the case of the clinotron. For simplicity assume that the function $f(z)$ in (4) is constant: $f(z)=1$. Also assume that perturbations in electron energy are small [$\gamma = \gamma_0 - \gamma_{(1)}$, where $|\gamma_{(1)}| \ll \gamma_0$], while the electron bunching caused by these perturbations can be significant. These assumptions reduce Eqs. (4) and (5) to

$$\frac{\partial\gamma_{(1)}}{\partial z'} = Ae^{-x_0+\alpha z'}\cos\vartheta, \tag{30}$$

$$\frac{\partial\vartheta}{\partial z'} = \delta + \frac{\gamma_{(1)}}{(\gamma_0^2-1)^{3/2}}. \tag{31}$$

Here we normalized x_0 and α to the absolute value of the transverse wave number by introducing $\bar{x}_0 = \kappa x_0$ and $\bar{\alpha} = \kappa\alpha$ [in (30) the bars are omitted], the detuning δ has the same meaning as above. Correspondingly, the efficiency (6) can be rewritten as

$$\eta = \frac{1}{\gamma_0 - 1}\frac{1}{\Delta}\int_{x_{0,\min}}^{x_{0,\min}+\Delta}\left\{\frac{1}{2\pi}\int_0^{2\pi}\gamma_{(1)}(z'_{\text{end}})d\vartheta_0\right\}dx_0. \tag{32}$$

Here we ignore the field nonuniformity in the wide (y) transverse direction. The interaction of electrons with the field ends when electrons hit the grating plate, i.e., at $z'_{\text{end}} = x_0/\alpha$. Thus, electrons with different transverse entrance coordinates have different interaction lengths.

Equations (30) and (31) are similar to known equations describing the physics of interaction between electrons and electromagnetic field in such devices as traveling-wave tubes and free-electron lasers. As known,[18,19] those equations for electron motion can be reduced to the equation for the nonlinear pendulum. In the case of Eqs. (30) and (31), this means introducing a new set of variables: $\gamma' = \gamma_{(1)}/\sqrt{A}(\gamma_0^2-1)^{3/4}$, $\xi = \sqrt{A}z'/(\gamma_0^2-1)^{3/4}$, $\delta' = (\gamma_0^2-1)^{3/4}\delta/\sqrt{A}$, and $\alpha' = (\gamma_0^2-1)^{3/4}\alpha/\sqrt{A}$. In new variables, these equations do not contain two parameters (A and γ_0) and have the following forms:

$$\frac{\partial\gamma'}{\partial\xi} = e^{-x_0+\alpha'\xi}\cos\vartheta, \tag{33}$$

$$\frac{\partial\vartheta}{\partial\xi} = \delta' + \gamma'. \tag{34}$$

Correspondingly, the efficiency given above by (32) can be rewritten as

$$\eta = \frac{(\gamma_0^2-1)^{3/4}}{\gamma_0 - 1}\sqrt{A}\,\hat{\eta}, \tag{35}$$

where the normalized efficiency $\hat{\eta}$ is given by

$$\hat{\eta} = \frac{1}{\Delta}\int_{x_0-\Delta/2}^{x_0+\Delta/2}\left\{\frac{1}{2\pi}\int_0^{2\pi}\gamma(\xi_{\text{end}})d\vartheta_0\right\}dx_0. \tag{36}$$

These simple equations are derived for a thick electron beam propagating at a small angle with respect to the grating plate, which they reach at $\xi_{\text{end}} = x_0/\alpha'$.

When the beam thickness is negligibly small (all electrons have the same transverse entrance coordinate x_0), one can reduce these equations further by introducing $\bar{\gamma} = \gamma' e^{x_0/2}$, $\bar{\xi} = \xi e^{-x_0/2}$, $\bar{\alpha} = \alpha' e^{x_0/2}$, and $\bar{\delta} = \delta' e^{x_0/2}$. This change of variables reduces (33) and (34) to

$$\frac{\partial\bar{\gamma}}{\partial\bar{\xi}} = e^{\bar{\alpha}\bar{\xi}}\cos\vartheta, \tag{37}$$

$$\frac{\partial\vartheta}{\partial\bar{\xi}} = \bar{\delta} + \bar{\gamma}. \tag{38}$$

Correspondingly, the efficiency can be characterized by its normalized value,

$$\bar{\eta} = \frac{1}{2\pi}\int_0^{2\pi}\bar{\gamma}(\bar{\xi}_{\text{end}})d\vartheta_0. \tag{39}$$

This set of equations contains only three normalized parameters that are proportional to the interaction length, initial detuning of synchronism between electrons and a slow wave and a tilting angle.

The results of the calculations for the clinotron with a thin electron beam are shown in Fig. 3 as contours of equal values of the normalized efficiency $\bar{\eta}$ in the plane of parameters "initial" detuning $\bar{\delta}$ versus normalized interaction length $\bar{\xi}_{\text{end}}$ for several values of the normalized tilt angle $\bar{\alpha}$. Here Fig. 3(a) ($\bar{\alpha}=0$) corresponds to the orotron with a beam parallel to the grating plate. At zero detuning or mismatch of synchronism between electrons and synchronous wave, the efficiency is zero as in all O-type electron devices. This efficiency is positive when electron velocity slightly exceeds the phase velocity of the wave, i.e., at negative $\bar{\delta}$'s [see definition of this detuning given above after (7)].

Two other figures, Figs. 3(b) and 3(c), characterize the clinotron operation for the tilting parameter $\bar{\alpha}$ equal to 0.1 and 0.2, respectively. These contours clearly demonstrate that the tilt of a beam results in significant enhancement of the efficiency. The fact that this normalized efficiency, which characterizes the efficiency of electron bunching, is larger than 1.0 is not important because the efficiency given by (35) contains a small parameter proportional to the square root of the rf field amplitude. In this regard, this set of equations is quite similar to the simplest set of nonlinear equations for the conventional TWT (Ref. 18) where the efficiency can be represented as the product of the normalized efficiency, which can be larger than 1.0, and the Pierce gain parameter, which has a small value; see also pages 164 and 165 of Ref. 20 with the reference to Slater's *"Microwave Electronics."* (Note that the relativistic gyrotron can also be described by similar equations.[21]) Coming back to Fig. 3, let us note that optimal parameters and the maximum normalized efficiency of a de-

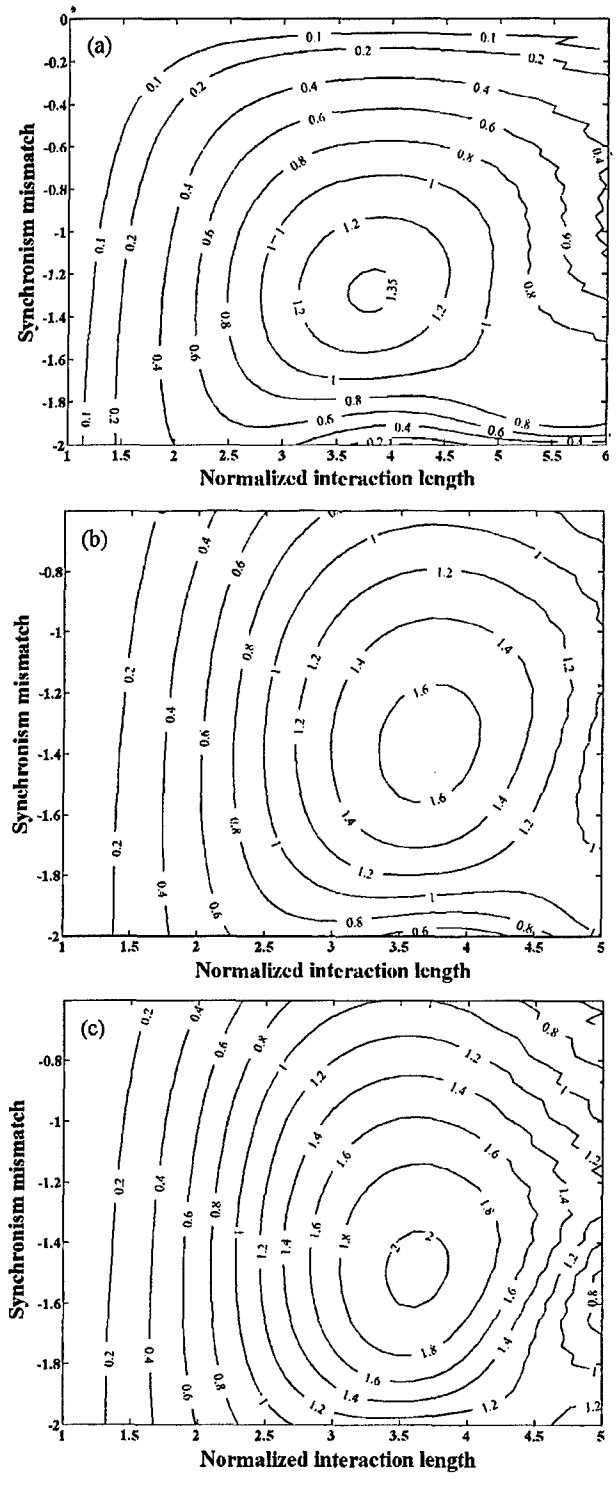

FIG. 3. Contours of constant values of the normalized efficiency in the plane of parameters "normalized initial detuning vs normalized interaction length" in the clinotron with different values of the tilt parameter $\bar{\alpha}$: (a) $\bar{\alpha}=0$, (b) $\bar{\alpha}=0.1$, and (c) $\bar{\alpha}=0.2$.

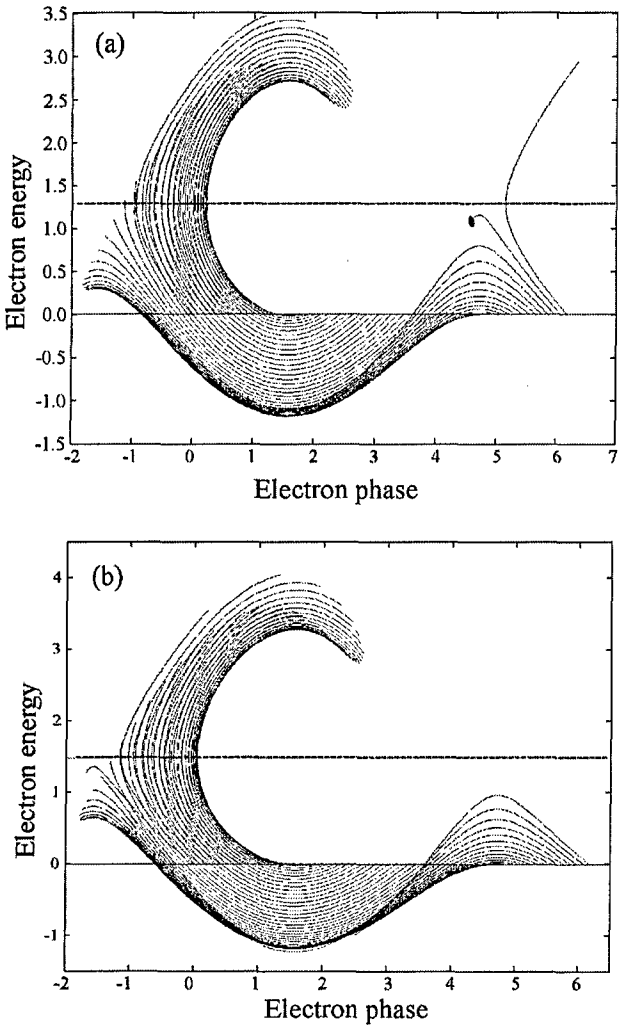

FIG. 4. Electron trajectories in the phase space "electron energy vs electron phase" in the clinotron with $\bar{\alpha}=0.1$ (a), and $\bar{\alpha}=0.2$ (b); the normalized initial detuning and the normalized interaction length have optimal values in accordance with Fig. 3(c).

vice with a parallel beam [Fig. 3(a), $\bar{\alpha}=0$] correspond to the results shown in Fig. 2(a) of Ref. 22.

Since we have mentioned above that the rf field amplitude plays here a role of a small parameter, it, possibly, makes sense to discuss the scaling of the efficiency and radiated microwave power with the operating voltage in more detail. In general, the balance equation for the power of microwave losses and the power withdrawn by the rf field from an electron beam can be written as

$$\frac{\omega}{Q}W=\eta V_b I_b. \tag{40}$$

Here the left-hand side represents the power of losses of the microwave energy $W=|A|^2V$ stored in the cavity having a volume V and the quality factor Q, while the right-hand side is the product of the interaction efficiency and the beam power V_bI_b. When the efficiency is given by (35), which at low voltages reduces to $\eta\propto(A^{1/2}/V_b^{1/4})\hat{\eta}$, the rf field amplitude, in accordance with (40), is proportional to $A\propto V_b^{1/2}I_b^{2/3}$. For electron guns with space-charge-limited emission this means $A\propto V_b^{3/2}$. Correspondingly, the efficiency (35) scales as $\eta\propto V_b^{1/2}\hat{\eta}$ and the radiated microwave power scales as $P_{\rm rf}\propto\hat{\eta}V_b^3$.

In Fig. 4, the electron trajectories are shown in the phase space of the set of Eqs. (37) and (38) for the optimal values

of the interaction length $\bar{\xi}_{end}$ and the detuning $\bar{\delta}$ for $\bar{\alpha}=0.1$ (a) and $\bar{\alpha}=0.2$ (b). The fact that decelerated particles move up in this figure corresponds to the representation of the electron energy as $\gamma=\gamma_0-\gamma_{(1)}$; our variable $\bar{\gamma}$ is proportional to $\gamma_{(1)}$. A thin solid horizontal line $\gamma=0$ is given for showing the initial positions of electrons whose phases at the entrance are uniformly distributed from 0 to 2π and perturbation in energy is equal to zero. The dashed horizontal line in this figure corresponds to $\bar{\gamma}=-\bar{\delta}$, which is the case when the changes in electron energy compensate for the initial mismatch of synchronism between the wave and electrons. As seen in Fig. 4, electrons, which start interaction in the decelerating phase, show some signs of over saturation to the end of interaction where their energy γ starts to decrease. Maximum changes in electron energy in case (b) are larger that corresponds to higher efficiencies shown in Fig. 3(c) than in Fig. 3(b). The exponential term in (37) causes the speeding up the deceleration process in the final stage of interaction. In a certain sense, this exponential term leading to the increase of electron coupling to the rf field in the process of interaction can be treated similarly to the known tapering of the depth of corrugations in a slow-wave structure resulting in the efficiency enhancement in backward-wave oscillators.[23,24] (Similar means of the efficiency enhancement are also known in the theory of free-electron lasers with variable parameters.)

The results of the calculations for the clinotron with a thick electron beam are shown in Fig. 5, which shows the degradation of the efficiency $\hat{\eta}$ with the beam thickness for several values of the normalized tilt angle α'. The calculations were done for the values of the mismatch of synchronism and the normalized interaction length optimal for a thin beam. Recall that normalization of all the variables and parameters in (37) and (39), and (33)–(36) is different and the results shown in Fig. 5 correspond to normalization adopted in (33)–(36) while those shown in Fig. 3 corresponded to normalization adopted in (37)–(39). As one can see, when the beam thickness reaches its maximum value, $\Delta_{max}=2x_0$ (here both Δ and x_0 are normalized to the absolute value of the transverse wave number κ), the efficiency is in the range of 0.5–0.6 of its maximum value for an ideally thin beam for all three values of α'.

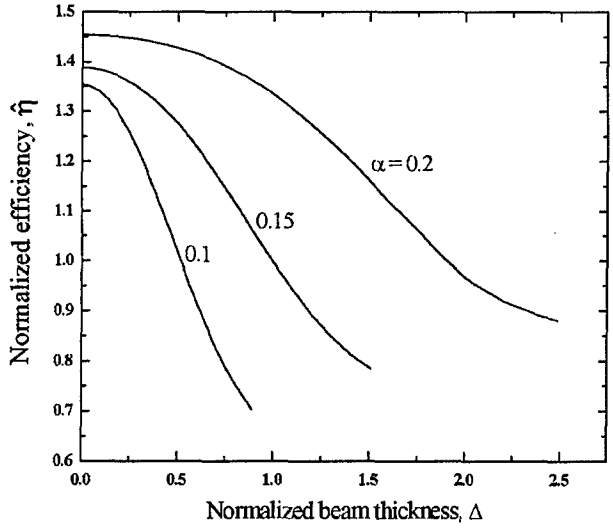

FIG. 5. Dependence of the clinotron efficiency on the beam thickness for several values of the tilt parameter α'.

V. DISCUSSION

It should be instructive to apply the simple formalism described above to a design where 1D and 2.5D simulations were done and compare the results. Consider for this purpose a recent design of a W-band (95 GHz) sheet-beam traveling-wave tube,[10] where 1D simulations predicted 24% efficiency, while 2.5D PIC simulations yielded the efficiency close to 22%. That design was done for a planar ridged waveguide geometry and a 120-kV electron beam of an elliptical cross section of 1 cm × 0.5 mm. The latter can be approximated by a rectangular cross section of the same size, and the variation of the rf field in the wide transverse direction will be neglected below.

From the condition of Cherenkov synchronism between electrons and the phase velocity of the wave, $v_{el}\approx v_{ph}=\omega/k_z$, one can easily find the axial wave number of the zero space harmonic synchronous with the traveling wave: $k_z\approx\omega/c\beta$. Correspondingly, the absolute value of the transverse wave number of this harmonic, $\kappa=(\omega/c)/\sqrt{\gamma_0^2-1}$, for a given voltage and frequency is close to 3.8 mm^{-1}. The transverse structure of the axial electric field in such a planar ridged waveguide can be given by $E_z=\cosh(\kappa x)$. Correspondingly, the coefficient C determined by Eq. (11) is equal to $C=(1/2)[1+\sinh(\kappa\Delta)/\kappa\Delta]$. For given $\kappa\approx3.8$ mm^{-1} and the beam thickness $\Delta=0.5$ mm, this coefficient is close to 1.378 and $C^2\approx1.9$. In turn, the coefficient D determined by (15) is equal to $D=(1/2)\{3/4+\sinh(\kappa\Delta)/\kappa\Delta+\sinh(2\kappa\Delta)/8\kappa\Delta\}$ that for given κ and Δ yields $D\approx1.99$. Thus, the ratio $I=C^2/D$ in this design is close to 0.955. Therefore, the transverse nonuniformity of the rf field should reduce the 24% efficiency calculated in 1D simulations to 22.9% that is a little higher than 22% efficiency obtained in PIC simulations.[10] This small discrepancy can be explained, first, by our neglect of the rf field nonuniformity in the wide horizontal direction and, second, by the fact that in PIC simulations, it was observed that in the region of efficient interaction the electrons exhibit strong pulsations in vertical direction, which make the vertical size of the beam in this region larger than initial 0.5 mm thickness.

VI. SUMMARY

A simple analytical theory is developed which describes the effect of the transverse nonuniformity of the interaction space on the efficiency of various sources of microwave radiation driven by linear electron beams. This issue seems to be especially important for novel sources of terahertz radiation where the beam thickness can be on the order or larger than the scale of transverse nonuniformity of the rf field. It is shown how to use this theory for evaluating the efficiency degradation in the case of cylindrical and sheet electron beams in various microwave circuits. The authors hope that this theory, while being unable to compete, will complement

well-elaborated numerical methods for detailed design of these devices and, hence, will be used for "zero-order" estimates of the efficiency degradation caused by the transverse nonuniformity of the rf field. Certainly, after minor modifications it can also be used for evaluation of the gain degradation in amplifiers with transversely nonuniform interaction space, since the gain can be presented as $G = 10 \log\{\eta P_b / P_{in}\}$, where P_b is the beam power and P_{in} is the input power from a driver.

ACKNOWLEDGMENT

This work is sponsored by the AFOSR MiPRI program.

[1]F. S. Rusin and G. D. Bogomolov, Proc. IEEE **57**, 720 (1969).
[2]D. E. Wortman and R. P. Leavitt, in *Infrared and Millimeter Waves*, edited by K. J. Button (Academic, New York, 1983), Vol. 7, Chap. 7.
[3]W. J. Pohl, IEEE Trans. Electron Devices **ED-12**, 351 (1965).
[4]K. R. Eppley, W. B. Herrmannsfeldt, and R. H. Miller, IEEE Particle Accelerator Conference, Washington, D.C., March 1987, Vol. 3, p. 1809.
[5]G. Caryotakis, G. Scheitrum, E. Jongewaard *et al.*, *High Energy Density Microwaves, Proceedings of the Fourth Workshop on High Power RF*, edited by R. M. Phillips, AIP Conf. Proc. No. 474 (AIP, New York, 1999), p. 59.
[6]B. E. Carlsten, Phys. Plasmas **9**, 5088 (2002).
[7]E. R. Colby, G. Caryotakis, W. R. Fowkes, and D. N. Smithe, *High Energy Density Microwaves, Proceedings of the Fourth Workshop on High Power RF*, edited by R. M. Phillips, AIP Conf. Proc. No. 474 (AIP, New York, 1999), p. 74.
[8]A. G. Luchinin and G. S. Nusinovich, Int. J. Electronics **57**, 827 (1984).
[9]G. Ya. Levin, A. I. Borodkin, A. Y. Kirichenko, A. Y. Usikov, and S. A. Churilova, *The Clinotron* (Naukova Dumka, Kiev, Ukraine, 1992).
[10]B. E. Carlsten, S. J. Russell, L. M. Earley, F. L. Krawczyk, J. M. Potter, P. Ferguson, and S. Humphries, IEEE Trans. Plasma Sci. **33**, 85 (2005).
[11]G. Nusinovich, M. Read, and L. Song, Phys. Plasmas **11**, 4893 (2004).
[12]M. Chodorow and C. Susskind, *Fundamentals of Microwave Electronics* (McGraw-Hill, New York, 1964), Sec. 3.6.
[13]G. S. Nusinovich, Int. J. Electronics **51**, 457 (1981).
[14]K. Schunemann and D. M. Vavriv, IEEE Trans. Electron Devices **46**, 2245 (1999).
[15]I. S. Gradshteyn and I. M. Ryzhik, *Table of Integrals, Series and Products* (Academic, New York, 2000).
[16]S. H. Gold and G. S. Nusinovich, Rev. Sci. Instrum. **68**, 3945 (1997).
[17]A. Karp, Proc. IRE **45**, 496 (1957).
[18]L. A. Weinstein, Radiotekh. Elektron. (Moscow) **2**, 883 (1957).
[19]N. Kroll, in *Novel Sources of Coherent Radiation*, Physics of Quantum Electronics Vol. 5, edited by S. F. Jacobs, M. Sargent III, and M. O. Scully (Addison- Wesley, Reading, MA, 1978), pp. 115–157.
[20]J. R. Pierce, *Traveling-Wave Tubes* (Van Nostrand, New York, 1950).
[21]N. S. Ginzburg and G. S. Nusinovich, Radiophys. Quantum Electron. **22**, 522 (1979).
[22]V. L. Bratman, N. S. Ginzburg, N. F. Kovalev, G. S. Nusinovich, and M. I. Petelin, in *Relativistic High-Frequency Electronics* (Inst. Appl. Phys., USSR Acad. Sci., Gorky, USSR, 1979), p. 249.
[23]N. F. Kovalev and V. I. Petrukhina, Electron. Techn. SVCh **7**, 101 (1977) (in Russian).
[24]L. D. Moreland, E. Schamiloglu, R. Lemke *et al.*, IEEE Trans. Plasma Sci. **22**, 554 (1994).

Analytical nonlinear theory of the orotron

Gregory S. Nusinovich
Institute for Research in Electronics and Applied Physics, University of Maryland, College Park, Maryland 20742-3511

(Received 27 February 2006; accepted 7 April 2006; published online 12 May 2006)

The orotron is a device in which a sheet electron beam excites electromagnetic (EM) oscillations in an open resonator formed by a concave mirror and a periodic grating plate. The first spatial harmonic of a field near the grating has phase velocity close to electron velocity; therefore electrons streaming over the grating surface produce Cherenkov or Smith-Purcell radiation. The orotrons can be configured for producing coherent radiation at short millimeter and submillimeter wavelengths (up to the terahertz range). Typically the amplitude of the EM field in the orotron is rather small. Therefore, for extracting an appreciable part of electron kinetic energy, it is necessary to realize synchronous interaction between electrons and a slow wave at long enough distances. This peculiarity of the orotron operation makes it possible to develop an analytical nonlinear theory of the orotron. Such a theory showing how to optimize the choice of the interaction length and the ratio between ohmic and diffractive losses is developed in the present paper. The theoretical treatment is accompanied with consideration of practical effects limiting the orotron efficiency.
 [DOI: 10.1063/1.2200631]

I. INTRODUCTION

At present, there is a strong interest in developing lightweight, compact, high-power sources of terahertz (THz) radiation for numerous applications. Although fast-wave devices, such as gyrotrons, cyclotron autoresonance masers, and free-electron lasers offer very high power level at short wavelengths, they do not satisfy requirements to the weight and compactness. Therefore, the decision should be made in favor of slow-wave devices. These devices can be configured as amplifiers and/or oscillators. Below we focus on oscillator configurations only. Among slow-wave oscillators operating at short millimeter and submillimeter wavelengths, the most known are backward-wave oscillators (BWOs), whose frequency can be voltage tunable in a wide range, and extended interaction oscillators (EIOs). The information on EIOs can be found on the web site of CPI, Canada, a well-known manufacturer of these devices. The power level of BWOs developed by the Russian corporation "Istok" varies from 1–10 mW at frequencies 260–375 GHz down to 0.5–2 mW at frequencies exceeding 1 THz.[1] This power level can be increased in the configuration of BWOs where an electron beam propagates at a small angle to the slow-wave circuit. Such configuration is known as the clinotron; the latest results of the development of clinotrons can be found in Ref. 2.

An alternative version of a compact oscillator, which can deliver significant power at wavelengths shorter than 1 mm, is the orotron (this name is an acronym for Russian words meaning "open resonator with reflecting grating").[3] A schematic of this device is shown in Fig. 1. In the orotron, electrons excite the electromagnetic (EM) field in an open resonator formed by a smooth concave mirror and a flat mirror with a periodic grating. Due to grating periodicity, the EM field contains spatial harmonics. So, electrons can propagate in Cherenkov synchronism with the phase velocity of the first harmonic and produce coherent Cherenkov or Smith-Purcell radiation. Typically, the EM field is excited in such a manner that the field of the zero space harmonics bounces back and forth between the flat and concave mirror (i.e., it has a small axial wave number), while the axial wave number of the first spatial harmonic is equal to $2\pi/d$, where d is the grating period. Thus, the condition of Cherenkov synchronism can be given as

$$v_{el} \simeq v_{ph} = \omega/k_z = cd/\lambda. \tag{1}$$

The advantage of the orotron is the presence of a high-Q resonator, which may allow one to excite EM oscillations even at a relatively low beam power. Just this fact had stimulated our interest in this device. At present, there are a large number of papers on the orotron; these papers were reviewed in Refs. 4–6. Recent experiments with submillimeter-wave orotrons[7] resulted in delivering up to 60 mW power at the 370-GHz frequency. Theoretical papers include the analysis of linear and nonlinear processes in one–dimensional (1D) and two–dimensional (2D) approximations (see, e.g., Ref. 6). Of course, with the use of presently available codes three–dimensional (3D) simulations also can be performed. The goal of the present paper, however, is completely different. Below we explain how one can estimate the orotron efficiency by very simple means. This method is based on the analytical theory originally developed for the gyrotron.[8,9] The paper is organized as follows. Section II contains the formalism describing the problem, results of analysis for an ideal electron beam, and discussion. In Sec. III the effect of electron velocity spread is considered. Section IV summarizes our paper.

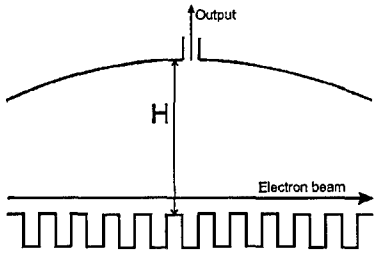

FIG. 1. Schematic of the classical orotron configuration.

II. GENERAL FORMALISM AND RESULTS FOR IDEAL ELECTRON BEAM

A. Formalism

There are two facts important for the theory developed below. First, at submillimeter wavelengths, a significant part of radiated EM energy can be lost in the resonator walls having finite conductivity (ohmic losses). Therefore, optimization of the orotron parameters should be done for maximizing the output efficiency

$$\eta_{\text{out}}=\left(1-\frac{Q}{Q_{\text{ohm}}}\right)\eta_{el}=\frac{1}{1+\hat{Q}}\eta_{el}, \tag{2}$$

instead of the electronic one, η_{el}. (In this regard, optimization of the orotron has something in common with optimization of gyrotrons at submillimeter wavelengths.[8–10]) In (2), $\hat{Q}=Q_D/Q_{\text{ohm}}$ is the ratio of the diffractive quality factor Q_D, which accounts for losses in the coupling hole shown in Fig. 1, to the ohmic quality factor Q_{ohm}; the total quality factor in (2) is determined by both kinds of losses, $1/Q=1/Q_D+1/Q_{\text{ohm}}$. The diffractive Q factor associated with the coupling hole can be evaluated as $Q_D=\omega W/P_{\text{rad}}$, where W is the EM energy stored in the resonator and P_{rad} is the EM power propagating via this hole. When diffractive losses due to finite sizes of both mirrors become important, Q_D should account for these losses as well (see, e.g., Ref. 11). These losses are important for the selection of modes with large numbers of field variations on mirrors.

Second, typically, at such short wavelengths, it is rather difficult even to fulfill the self-excitation conditions; thus, the device operates at currents which exceed the start current only slightly. This means that the amplitude of EM oscillations in such a device is rather small—much smaller than the optimal for the interaction efficiency. To compensate for this smallness, it is expedient to increase the interaction length. Then, at least, efficient bunching in the process of interaction may take place that should result in the efficiency enhancement in comparison with a device of a shorter length.

Let us illustrate the consequences from this fact (small EM amplitude, long interaction length) with the use of equations for electron motion and the balance equation for the EM power produced by an electron beam and the power of EM losses in a cavity. For simplicity, we will ignore the electron velocity spread and the transverse nonuniformity of the interaction space (these factors will be discussed later). As shown elsewhere,[12] 1D electron motion in a resonator, where electrons are in synchronism with one of the spatial harmonics of an EM filed, can be described by two first-order equations for normalized electron energy $\gamma=\varepsilon/mc^2$ and slowly variable phase $\vartheta=\omega t-k_z z$,

$$\frac{\partial\gamma}{\partial z'}=-\text{Re}\{\alpha_1 f(z')e^{i\vartheta}\}, \tag{3}$$

$$\frac{\partial\vartheta}{\partial z'}=\frac{\gamma}{\sqrt{\gamma^2-1}}-h. \tag{4}$$

In (3) and (4), we introduced a number of normalized parameters: the normalized axial coordinate $z'=\omega z/c$, the normalized amplitude of the first spatial harmonic of the EM field $\alpha_1=eA_1/mc\omega$ (the function $f(z')$ describes its axial structure), and the normalized axial wave number $h=k_z c/\omega$, which is the inverse phase velocity of the first spatial harmonic normalized to the speed of light. Also, the first term in the right-hand side (RHS) of (4), $1/\beta$ ($\beta=v_{el}/c$ is the electron velocity normalized to the speed of light), was written with the account for the general relation between the electron velocity and energy, $\gamma=1/\sqrt{1-\beta^2}$. The boundary conditions at the entrance are $\gamma(z'=0)=\gamma_0$, $\vartheta(z'=0)=\vartheta_0$, where initial phase ϑ_0 is uniformly distributed from 0 to 2π.

In these notations, the electronic efficiency can be determined as

$$\eta_{el}=\frac{1}{\gamma_0-1}\left\{\gamma_0-\frac{1}{2\pi}\int_0^{2\pi}\gamma(L')d\vartheta_0\right\}. \tag{5}$$

Here $L'=\omega L/c$ is the normalized interaction length. The balance equation can be given as

$$\frac{\omega}{Q}W=\eta_{el}P_b. \tag{6}$$

Here $P_b=I_bV_b$ is the beam power. Beam voltage, V_b, and the normalized initial energy of electrons, γ_0, are related as $\gamma_0=1+eV_b/mc^2$. Since the amplitude of the zero spatial harmonic, A_0, is typically much larger than amplitudes of other harmonics, the EM energy stored in the resonator volume V can be determined as $W\simeq(A_0^2/8\pi)V$.

When perturbations caused by the EM field in both the electron energy and phase are small, one can readily get from (3)–(6) the starting conditions, which determine the start current of the device (such current was analyzed elsewhere[13]). Below we consider the situation when the beam current slightly exceeds its starting value. In such a case the oscillations are excited with small amplitude. Hence, in (4), we can treat changes in the electron energy in the process of interaction as perturbations ($\gamma=\gamma_0-\tilde{\gamma}$, where $|\tilde{\gamma}|\ll\gamma_0$), while the changes in phase can be significant at a long enough distance. Under these assumptions, Eqs. (3) and (4) can be rewritten as

$$\frac{\partial\tilde{\gamma}}{\partial z'}=\text{Re}(\alpha_1 f(z')e^{i\vartheta}), \tag{7a}$$

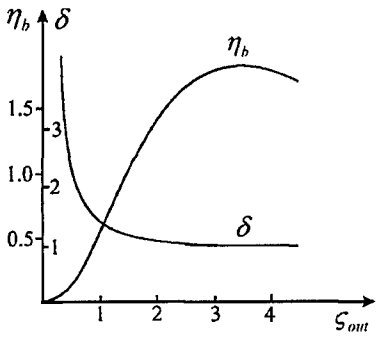

FIG. 2. Electron bunching efficiency η_b and optimal detuning δ as functions of the normalized interaction length ς_{out}.

$$\frac{\partial \vartheta}{\partial z'} = \frac{1}{\beta_0} - h + \frac{\tilde{\gamma}}{(\gamma_0^2 - 1)^{3/2}} \tag{7b}$$

and, hence, these two equations can be reduced to one nonlinear pendulum-like equation,

$$\frac{\partial^2 \vartheta}{\partial z'^2} = \frac{1}{(\gamma_0^2 - 1)^{3/2}} \mathrm{Re}\{\alpha_1 f(z') e^{i\vartheta}\}. \tag{8}$$

The amplitude of the first spatial harmonic α_1 as well as the function $f(z')$ describing its axial structure can be assumed real. Then, introducing a new normalized axial coordinate $\varsigma = \sqrt{\alpha_1/(\gamma_0^2-1)^{3/2}} z'$, we can reduce (8) to

$$\frac{\partial^2 \vartheta}{\partial \varsigma^2} = f(\varsigma)\mathrm{Re}(e^{i\vartheta}). \tag{9}$$

This equation should be supplemented with the boundary conditions at $\varsigma=0$ for the electron phase $(\vartheta(0)=\vartheta_0 \in [0;2\pi])$ and its derivative $\partial\vartheta/\partial\varsigma|_{\varsigma=0}=\delta$, where $\delta = (1/\beta_0 - h)/\sqrt{\alpha_1/(\gamma_0^2-1)^{3/2}}$ is the normalized initial detuning, which is the same for all electrons in an ideal (zero velocity spread) electron beam.

Equation (7b) shows that the changes in electron energy are proportional to the phase derivative. Therefore, the electronic efficiency (5) can be rewritten as

$$\eta_{el} = \left[\frac{(\gamma_0+1)^3}{\gamma_0 - 1}\right]^{1/4} \sqrt{\alpha_1} \left\{ \frac{1}{2\pi} \int_0^{2\pi} \left.\frac{\partial \vartheta}{\partial \varsigma}\right|_{\varsigma_{out}} d\vartheta_0 - \delta \right\}. \tag{10}$$

The expression in figure brackets characterizes the electron bunching. Therefore it will be called below the bunching efficiency and denoted by η_b. As shown elsewhere,[9,14] its value can be larger than 1. This efficiency optimized with respect to the normalized detuning is shown as the function of the normalized interaction length for the device with a Gaussian axial structure of the EM field in Fig. 2 reproduced from Ref. 14. (Here, the Gaussian distribution corresponds to the case when at the entrance and the exit the field amplitude is e times smaller than in the middle of the resonator.) It should be emphasized that because of increasing the interaction length, the electronic efficiency (10) scales at small amplitudes as $\sqrt{\alpha_1}$, while in devices of a fixed length it scales as α_1^2 (see, e.g., Ref. 12). The expression in square brackets in (10), at low voltages, reduces to $[(\gamma_0+1)^3/(\gamma_0-1)]^{1/4} \simeq (8mc^2/eV_b)^{1/4}$. Note that, as the voltage reduces, the EM field amplitude reduces as well, as follows from the balance equation.

In accordance with the steps made, the balance equation (6) can be rewritten as

$$\alpha_1 = \hat{I} \frac{\hat{Q}}{1+\hat{Q}} \frac{\eta_b}{\varsigma_{out}}. \tag{11}$$

Here the normalized current parameter $\hat{I}$ is equal to

$$\hat{I} = \frac{2}{\pi} Q_{ohm} \frac{ej\lambda^2}{mc^3} \frac{\alpha_1^2}{\alpha_0^2} \frac{w_v}{H}. \tag{12}$$

In (12), j is the electron current density in the interaction space, α_0 is the amplitude of the zero spatial harmonic of the EM field normalized in the same fashion as α_1 above. The last ratio w_v/H is the ratio of the thickness of a sheet electron beam in the vertical direction, w_v, to the distance H between two mirrors shown in Fig. 1. In transforming (6) into (11) we took into account not only normalization of a new variable ς_{out}, but also the fact that the resonator volume increases with the length, as the amplitude of EM oscillations gets smaller. It was also assumed that the beam horizontal width is equal to the resonator size in the direction perpendicular to the schematic shown in Fig. 1.

So, Eqs. (2) and (9)–(11) form a set of equations, which can be used for optimizing the Q ratio $\hat{Q}$ and the normalized interaction length ς_{out} for maximum output efficiency.

B. Results and discussion

Optimization with respect to the Q ratio readily yields the optimum value

$$\hat{Q}_{opt} = 1/2. \tag{13}$$

This value, obtained with the account for the dependence of the EM field amplitude α_1 on the Q ratio given by (11), shows that 1/3 of the radiated microwave power should be lost in the resonator walls, while 2/3 can be extracted via a coupling hole shown in Fig. 1.

Optimization of the normalized length should be done with the use of Eqs. (2), (10), and (11). From (11) it follows that

$$\frac{d\alpha_1}{d\varsigma_{out}} = \frac{\hat{Q}}{1+\hat{Q}} \hat{I} \frac{d}{d\varsigma_{out}} \left(\frac{\eta_b}{\varsigma_{out}}\right), \tag{14}$$

while optimization of the output efficiency with respect to this length yields

$$\sqrt{\alpha_1} \frac{d\eta_b}{d\varsigma_{out}} + \frac{1}{2\sqrt{\alpha_1}} \eta_b \frac{d\alpha_1}{d\varsigma_{out}} = 0. \tag{15}$$

With the use of (14) and (11), Eq. (15) can be reduced to[9]

$$\left(\frac{s_{\text{out}}}{\eta_b}\frac{d\eta_b}{ds_{\text{out}}}\right)_{\text{opt}}=\frac{1}{3}. \tag{16}$$

For the case of the Gaussian axial structure of the EM field, solution of (16) can be found with the use of Fig. 2. It is $s_{\text{out,opt}}=2.65$; the corresponding value of the bunching efficiency is equal to 1.78. As is seen in Fig. 2, this normalized length is smaller than the one optimal for the bunching efficiency.

For these optimal values of the Q ratio and normalized interaction length, the normalized amplitude of the first spatial harmonic of the EM field is equal to $\alpha_{1,\text{opt}}\simeq 0.224\hat{I}$, and the maximum output efficiency is equal to

$$\eta_{\text{out,max}}\simeq 0.56\hat{I}^{1/2}. \tag{17}$$

So, the results of our optimization show that the maximum output efficiency depends on the normalized beam current parameter defined by (12). Most of the parameters in (12) are essentially the same as those analyzed in Refs. 13 and 15, which allows us to make use of the analysis done there. In particular, it was found[15] that the maximum ratio of the amplitude of the first spatial harmonic to that of the zeroth one can be achieved when the grooves shown in Fig. 1 are a quarter-wavelength deep and their width is equal to half of the period d. In such a case, the ratio α_1/α_0 in (12) is equal to $2/\pi$. Also, the ohmic Q factor in such a case, as shown in,[15] is equal to

$$Q_{\text{ohm}}=\frac{H}{\delta_{sk}\left(3+\dfrac{\lambda}{d}\right)}. \tag{18}$$

Here δ_{sk} is the skin depth, which we, for practical reasons, will take equal to twice its theoretical value $\delta_{sk}^{th}=(1/2\pi)\sqrt{\lambda c/\sigma}$ (σ is the wall conductivity). Equation (18) is very important. In the absence of grooves, the ohmic Q factor of a resonator formed by two smooth plates is equal to $Q_{\text{ohm}}=H/2\delta_{sk}$. Comparison of this formula with (18) shows that the presence of grooves reduces the ohmic Q by the factor of $(3+\lambda/d)/2$. Once we take into account that, in accordance with the Cherenkov synchronism condition (1), $\lambda/d\simeq 1/\beta_0$, we come to the conclusion that just a large number of deep and narrow grooves forming a grating plate plays the crucial role in the enhancement of ohmic losses. So, below we will determine the ohmic Q factor as

$$Q_{\text{ohm}}\simeq\frac{H}{\delta_{sk}}\frac{\beta_0}{1+3\beta_0}, \tag{18a}$$

because (18a) better illustrates the consequences of lowering the beam voltage for the device performance. At low voltages, the normalized electron velocity is equal to $\beta_0\simeq\sqrt{2eV_b/mc^2}\simeq\sqrt{V_b(kV)}/16$.

Lastly, the thickness of a beam in the vertical direction, w_v, should be small enough for avoiding efficiency degradation because of the vertical nonuniformity of the slow wave localized near the grating. As shown in Ref. 12, this degradation becomes important (the efficiency degrades by a factor of 2) when the beam thickness is on the order of $\lambda\beta_0/\pi$. So, expressing the distance between mirrors, H, in terms of half wavelengths, $H\simeq q(\lambda/2)$, where index q shows the number of field variations in the vertical direction, the ratio w_v/H in (12) can be estimated as $2\beta_0/\pi q$. With all this in mind, the expression for the normalized current parameter (12) can be rewritten as

$$\hat{I}=\frac{8}{\pi^4}\frac{\lambda}{\delta_{sk}}\frac{ej\lambda^2}{mc^3}\frac{\beta_0^2}{1+3\beta_0}. \tag{19}$$

This equation shows that to maintain the value of this parameter fixed as the wavelength shortens the beam current density should increase inversely proportional to $\lambda^{5/2}$. Also, it follows from (19) that at low voltages (when $3\beta_0\ll 1$) the beam current parameter $\hat{I}$ is linearly proportional to the beam voltage.

To illustrate the meaning of this equation, let us consider an example: the wavelength equal to 0.8 mm (at this wavelength, the skin depth for copper is close to $0.22\cdot 10^{-4}$ cm), the beam voltage equal to 4 kV, and the beam current density equal to 30 A/cm^2. For these numbers, the normalized beam current given by (19) is equal to $0.38\cdot 10^{-4}$. (The thickness of such a beam in vertical direction should not exceed 32 μm.) This value of the normalized beam current corresponds to the normalized amplitude of the first spatial harmonic of the EM field equal to $0.85\cdot 10^{-5}$. For a given voltage and this amplitude, the optimal normalized length $s_{\text{out,opt}}=2.65$ corresponds to the ratio of the interaction length to the wavelength $L/\lambda\simeq 6.4$. For such small amplitude, the maximum output efficiency given by (17) is close to 0.35% only. Of course, the total radiated microwave power increases with the width of a system in a wide horizontal direction. For instance, when this width is equal to 3 mm, the total beam current is about 30 mA. Correspondingly, the beam power is 120 W and the power of outgoing radiation is 0.42 W. Recall that here we consider the beam current density in the interaction space, which can be increased by compressing a beam in the transition region between electron gun and the interaction space, when such a region exists. For instance, if the current density is increased due to beam compression from 30 A/cm^2 taken above to 300 A/cm^2, the beam current parameter $\hat{I}$ (19) also becomes 10 times larger, which increases the output efficiency (17) from 0.35% to about 1.1%. Correspondingly, the total power of radiation increases from 0.42 to 13 W. (Now we assume that the total beam current is 0.3 A.)

The beam compression can, in particular, be realized in miniaturized plasma-cathode electron guns[16] suitable for short-wavelength applications. Originally, similar guns[17] were developed for plasma-assisted microwave oscillators.[18] In such guns, the beam compression can be realized by proper axial profiling of the neutral gas density, because impact ionization of these neutrals by a propagating electron beam produces the ions providing ion focusing of the beam.

III. EFFECT OF ELECTRON VELOCITY SPREAD

The method proposed has some limitations once the spread in electron velocities is taken into account. Let us come back to the equation for the slowly variable phase (4)

and determine the limitation on the interaction length caused by electron velocity spread.

The equation for a slowly variable phase (4) can be rewritten as

$$\frac{\partial \vartheta}{\partial z'} = \frac{1}{\beta} - \frac{1}{\beta_{ph}}, \tag{20}$$

where β_{ph} is the phase velocity of the first spatial harmonic of the wave normalized to the speed of light. Above we were focused on the effect of changes in the electron velocity and energy in the process of interaction on the phase bunching. Now, let us evaluate the effect of the spread in initial velocities on the synchronism between electrons and the wave. In accordance with (20), electrons having initial normalized velocity different from the mean value $\bar{\beta}_0$, say $\beta_0 = \bar{\beta}_0 + \Delta\beta_0$, experience additional phase shift, which can be evaluated as $\Delta\vartheta = (-1/\bar{\beta}_0)(\Delta\beta_0/\bar{\beta}_0)z'$. Assume that the velocity spread is acceptable when all electrons stay in approximately the same phase with respect to the wave, i.e., when the phase shift caused by the velocity spread does not exceed $\pi/2$. This limitation immediately gives us the maximum ratio of the interaction length to the wavelength

$$\frac{L_{\max}}{\lambda} = \frac{\bar{\beta}_0}{4\delta\beta_0}, \tag{21}$$

where $\delta\beta_0 = \Delta\beta_0/\bar{\beta}_0$ is the relative spread, which can be given in percents. Taking into account the Cherenkov synchronism condition (1), Eq. (21) can be rewritten in terms of the number of grating periods $N = L/d$ as

$$N_{\max} = 1/4\,\delta\beta_0. \tag{21a}$$

So, as follows from (21a), for instance, in the case of 1% velocity spread the maximum number of periods is equal to 25. Coming back to the optimal ratio $L/\lambda \simeq 6.4$ found in the example considered above, we can conclude that for realizing this ratio the velocity spread should not exceed 0.5%.

This issue can be analyzed in a more general manner with the use of the formalism developed above. Combining the optimal value of the normalized amplitude of the first harmonic of the EM field, $\alpha_{1,\mathrm{opt}} \simeq 0.224\hat{I}$, with the optimal value of the normalized length $\varsigma_{\mathrm{out,opt}} = 2.65$ and the limitation on the interaction length given by (21) or (21a), one can readily find that to fulfill this limitation the electron current density in the interaction space should obey the following condition:

$$\frac{\lambda}{\delta_{sk}} \frac{ej\lambda^2}{mc^3} \frac{\bar{\beta}_0}{1+3\bar{\beta}_0} > 155(\delta\beta_0)^2. \tag{22}$$

When this condition cannot be fulfilled, the interaction length should be chosen in accordance with (21), while the normalized amplitude will be determined by the beam current, in accordance with the balance equation (11). As a result, the normalized length ς_{out} will be smaller than its optimal value found above and, correspondingly, the output efficiency will be smaller than its optimal value.

To enhance the interaction efficiency, one can consider a two-stage device, where in the first stage, whose length obeys restrictions (21) and (21a) and whose grating period is constant, the electron bunch is formed. Then, deceleration of this bunch takes place in the second stage where the grating period varies with distance. This concept of a device with tapered parameters is known in traveling-wave tubes[19] and in free-electron lasers.[20,21] The wall-plug efficiency of such low-efficiency devices, of course, can also be greatly increased by using depressed collectors. This means, however, complicates the device and increases its weight and sizes.

IV. SUMMARY

A simple theory presented in this paper allows developers to easily evaluate the efficiency and the most important constraints in the design of the orotrons intended for operation at submillimeter wavelengths, up to the THz range. As follows from the results presented, two of the most critical issues for operation at such high frequencies are the ohmic losses in small-period gratings and relatively low electron current density. To solve the first problem, a variety of alternative concepts of periodic structures can be proposed and analyzed. Manufacturing of such structures, when necessary, can be done with the use of novel methods of microfabrication (see, e.g., Ref. 22). Thus, the structures, which seemed unrealistic some time ago, can be revisited today. To solve the problem of low current density, new emitters with high current density as well as methods of beam compression requiring a careful design of electron optical systems with the use of presently available numerical codes, should be used.

ACKNOWLEDGMENT

This work is supported by the Air Force Office of Scientific Research (Microwave Power Research Initiative—MiPRI).

[1] A. A. Negirev, "Wide bandwidth BWO's continuously covering millimeter- and submillimeter-wavelength ranges," in *Vacuum Microwave Electronics* (Institute of Applied Physics, Nizhniy Novgorod, 2002) (in Russian).
[2] D. M. Vavriv, in *High Energy Density and High Power RF: 7th Workshop*, AIP Conf. Proc. No. 807, edited by D. K. Abe and G. S. Nusinovich (AIP, New York, 2006), p. 367.
[3] F. S. Rusin and G. D. Bogomolov, JETP Lett. **4**, 236 (1966); Proc. IEEE **57**, 720 (1969).
[4] D. E. Wortman and R. P. Leavitt, in *Infrared and Millimeter Waves*, edited by K. J. Button (Academic, New York, 1983), Vol. 7, Part II, Chap. 7.
[5] L. A. Weinstein, V. A. Isaev, and D. I. Trubetskov, Radiotekh. Elektron. (Moscow) **28**, 1233 (1983).
[6] M. B. Tseitlin and E. A. Myasin, Radiotekh. Elektron. (Moscow) **38**, 961 (1993).
[7] V. L. Bratman, I. V. Bandurkin, B. S. Dumesh, A. E. Fedotov, Y. K. Kalynov, N. G. Kolganov, V. N. Manuilov, F. S. Rusin, S. V. Samsonov, and A. V. Savilov, in *High Energy Density and High Power RF: 7th Workshop*, AIP Conf. Proc. No. 807, edited by D. K. Abe and G. S. Nusinovich (AIP, New York, 2006), p. 356.
[8] G. S. Nusinovich, in *Infrared and Millimeter Waves*, edited by K. J. Button (Academic Press, Orlando, 1984), Vol. 11, Part III, Chap. 6.
[9] G. S. Nusinovich, Elektronnaya Tekhn., Ser. I, Elektronika SVCh, No. 1, 16 (1981).
[10] R. J. Temkin, K. Kreischer, S. M. Wolfe, D. R. Cohn, and B. Lax, J. Magn. Magn. Mater. **11**, 368 (1979).
[11] L. A. Weinstein, *Open Resonators and Open Waveguides* (Golem, Boulder, CO, 1969), Secs. 15 and 41.
[12] G. S. Nusinovich and O. V. Sinitsyn, Phys. Plasmas **12**, 093107 (2005).

[13]F. S. Rusin and G. D. Bogomolov, Radiophys. Quantum Electron. **11**, 430 (1968).
[14]V. L. Bratman, N. S. Ginzburg, N. F. Kovalev, G. S. Nusinovich and M. I. Petelin, "Common properties of HF devices with prolonged inertial bunching of electrons," in *High-Frequency Relativistic Electronics*, edited by A. V. Gaponov-Grekhov (Institute of Applied Physics, Gorky, USSR, 1979), pp. 249–274.
[15]F. S. Rusin and G. D. Bogomolov, "Oscillating system of the orotron," in *High Power Electronics*, edited by P. L. Kapitsa and L. A. Weinstein (Nauka, Moscow, USSR, 1968), Vol. 5, p. 38
[16]J. Rodgers, R. Chang, V. Granatstein, T. Antonsen, Jr., G. Nusinovich, and Y. Carmel, IEEE Conf. Record—Abstracts (ICOPS-2005, Monterey, CA), paper 1B7, p. 101.
[17]D. M. Goebel and R. W. Schumacher, Patent No. 5,537,005 (16 July 1996).
[18]D. M. Goebel, J. M. Butler, R. W. Schumacher, J. Santoru, and R. L. Eisenhart, IEEE Trans. Plasma Sci. **22**, 547 (1994).
[19]J. G. Meeker and J. E. Rowe, IRE Trans. Electron Devices **9**, 257 (1962).
[20]N. M. Kroll, P. L. Morton, and M. N. Rosenbluth, IEEE J. Quantum Electron. **QE-17**, 1436 (1981).
[21]P. Sprangle, C.-M. Tang and W. M. Manheimer, Phys. Rev. A **21**, 302 (1980).
[22]G. P. Scheitrum, in *Modern Microwave and Millimeter-Wave Power Electronics*, edited by R. J. Barker, J. H. Booske, N. C. Luhmann, Jr., and G. S. Nusinovich (IEEE —Wiley Interscience, 2005), Chap. 7.